Lipid compound classes display diverging hydrogen isotope responses in lakes along a nutrient gradient

S. Nemiah Ladd[a, b]*, Daniel B. Nelson[a], Carsten J. Schubert[a], Nathalie Dubois[b,c]

[a] Swiss Federal Institute of Aquatic Science and Technology (EAWAG), Department of Surface Waters – Research and Management, Seestrasse 79, 6047 Kastanienbaum, Switzerland; Nemiah.Ladd@eawag.ch, Daniel.Nelson@eawag.ch, Carsten.Schubert@eawag.ch

[b]Swiss Federal Institute of Technology (ETH-Zürich), Department of Earth Sciences, Sonneggstrasse 5, 8092 Zürich, Switzerland

[c]Swiss Federal Institute of Aquatic Science and Technology (EAWAG), Department of Surface Waters – Research and Management, Überlandstrasse 133, P.O. Box 611, 8600 Dübendorf, Switzerland; Nathalie.Dubois@eawag.ch

*Corresponding author: Nemiah.Ladd@eawag.ch, +41 58 765 2223

Abstract

Compound specific hydrogen isotope ratios ($^2H/^1H$) of lipid biomarkers preserved in sediments are used as a paleohydrologic proxies. However, several variables, including contributions from different source organisms and their growth rates, can influence $^2H/^1H$ fractionation between lipids and source water. Significant uncertainties remain about how these factors combine to produce the net $^2H/^1H$ signal exported to sediments.

To assess the influence of phosphorus availability on $^2H/^1H$ ratios of lipids accumulating in lake sediments, we analyzed surface sediments and sediment traps from ten central Swiss lakes, representing a wide range of trophic states. In agreement with results from laboratory cultures, $^2H/^1H$ fractionation for the diatom biomarker brassicasterol (24-methyl cholest-5,22-dien-3β-ol) increased in more productive lakes (0.6 ± 0.1 ‰ per µg/L total P in sediment traps and surface sediments). In contrast, $^2H/^1H$ fractionation for phytol, the isoprenoid side-chain moiety of chlorophyll, decreased with increasing total P (-0.4 ± 0.1 ‰ per µg/L total P in sediment traps), suggesting that different biochemical mechanisms are responsible for changes in $^2H/^1H$ fractionation for each class of isoprenoidal lipids. Opposing changes in ^2H-fractionation for sterols and phytol cause their $^2H/^1H$ ratios to converge as total P increases. This response may be a new tracer for phytoplankton growth conditions and is not influenced by the source water isotope value.

Interpreting the $^2H/^1H$ ratios of short to long chain ($C_{14} – C_{30}$) *n*-alkanoic acids and *n*-alkanols is complicated by likely contributions from heterotrophs and/or vascular plants. These values generally did not correlate with lake water isotopes, nor did their fractionation factors correlate with total P. For most lipids there was no significant difference between sediment trap and surface sediment $^2H/^1H$ ratios. However, *n*-C_{14} – *n*-C_{18} fatty acids were ^2H-enriched in the surface sediments, most likely due to degradation in the water column. Our results indicate that interpretations of short-chain fatty acids as a water isotope signal likely require supporting information about ecological conditions and community structure, but that paired H isotope measurements of phytoplankton-derived sterols and phytol may be developed as a proxy for phytoplankton growth.

Key words: Hydrogen isotopes, lipid biomarkers, eutrophication, phosphorus, phytoplankton productivity, lacustrine sediment

1. Introduction

The distributions and stable isotope compositions of lipid biomarkers preserved in lacustrine and marine sediments can provide valuable information about past environmental and climatic conditions (Castañeda and Schouten, 2011; Sachse et al., 2012; Sessions, 2016). In recent years, compound specific hydrogen isotope measurements of leaf waxes have garnered considerable attention as a paleohydrologic proxy, since sedimentary leaf wax δ^2H values ($\delta^2H = \delta D = (({}^2H/{}^1H_{Sample})/({}^2H/{}^1H_{VSMOW}) - 1)$) are well correlated with δ^2H values of local precipitation over large spatial scales (Sachse et al., 2004; Sachse et al., 2012). Precipitation δ^2H values vary by location in response to temperature, amount of precipitation, and atmospheric moisture transport pathways (Dansgaard, 1964; Craig and Gordon, 1965; Gat, 1996). Although there are complications relating to plant type, timing of leaf wax synthesis, and evaporative enrichment of leaf water, extensive studies in modern systems have helped to constrain sources of uncertainty and enhanced the utility of the leaf wax hydrogen isotope proxy (Sachse et al., 2012; Kahmen et al., 2013; Tipple et al., 2013; Ladd and Sachs, 2015; Feakins et al., 2016; Freimuth et al., 2017; Nelson et al., 2018).

Compared to the existing body of work on leaf wax δ^2H values, considerably less has been done to understand the biologic complexity associated with aquatically sourced lipid δ^2H values. Lipids produced by aquatic organisms have δ^2H values that have been observed to correlate with δ^2H_{Water} in a range of natural and laboratory settings (reviewed by Sachse et al., 2012 and Sachs, 2014), which has led to the use of aquatic lipid δ^2H values as a proxy of past lake water isotope values (Huang et al., 2002; Sachs et al, 2009; Smittenberg et al., 2011; Nelson and Sachs, 2016; Randlett et al., 2017) and to the pairing of aquatic and leaf wax δ^2H values from the same sediment to reconstruct changes in relative humidity (Rach et al., 2014; Rach et al., 2017).

Previous work has demonstrated that fractionation factors between lipids and source waters (denoted by $\alpha_{Lipid\text{-}Water} = ({}^2H/{}^1H_{Lipid})/({}^2H/{}^1H_{Water})$) are not constant among compounds or among photoautotrophic aquatic species (Sessions et al. 1999; Schouten et al., 2006; Zhang and Sachs, 2007; Chivall et al., 2014; M'Boule et al., 2014; Heinzelmann et al., 2015). Additionally, environmental factors including salinity,

102 temperature, nutrient availability, and light availability can influence the magnitude of
103 $\alpha_{Lipid\text{-}Water}$ values in cyanobacteria and eukaryotic algae (Schouten et al., 2006; Sachs,
104 2014 and references therein; Nelson and Sachs, 2014; van der Meer et al., 2015;
105 Wolhowe et al., 2015; Maloney et al., 2016; Weiss et al., 2017; Sachs et al., 2017).
106 Furthermore, in the case of short-chained fatty acids that are synthesized by
107 heterotrophs, chemoautotrophs, and photoautotrophs, the central metabolic pathway
108 employed can have a much larger effect on δ^2H_{Lipid} values than any variability
109 observed in response to environmental gradients (X. Zhang et al., 2009; Osburn et al.,
110 2011; Heinzelmann et al., 2015). Disentangling the competing influence of different
111 factors on the net δ^2H_{Lipid} value exported to and preserved in sediments is necessary for
112 robust interpretations of down core δ^2H_{Lipid} values.
113 In particular, the role that lacustrine trophic status might play on sedimentary
114 δ^2H_{Lipid} values warrants more attention (Schwab et al., 2015; Ladd et al., 2017). There
115 are several reasons a lake's trophic status could influence δ^2H_{Lipid} values, the first of
116 which is by facilitating higher algal growth rates. In cultures of eukaryotic marine
117 algae, higher growth rates correlate with a decrease in $\alpha_{Lipid\text{-}Water}$ values for sterols,
118 alkenones, and some fatty acids, indicating more $^2H/^1H$ fractionation (Schouten et al.,
119 2006; Z. Zhang et al., 2009; Sachs and Kawka, 2015; Wolhowe et al., 2015).
120 Consistent with this result, $\alpha_{Lipid\text{-}Water}$ values from the diatom biomarker brassicasterol
121 (24-methyl cholest-5,22-dien-3β-ol) produced in the surface water of a eutrophic lake
122 in central Switzerland were lower than those of brassicasterol in a nearby oligotrophic
123 lake (Ladd et al., 2017). There was, however, no significant difference in $\alpha_{Lipid\text{-}Water}$
124 values for short-chain fatty acids and phytol between the two lakes (Ladd et al., 2017).
125 Another way that trophic status could influence sedimentary δ^2H_{Lipid} values is
126 by changing the algal community. Different nutrient regimes promote the growth of
127 different species of algae (Tilman et al. 1982; Jensen et al., 1994; Watson et al., 1997;
128 Monchamp et al., 2018). This diversity could complicate the δ^2H_{Lipid} signal of
129 compounds common to all photoautotrophs, since $\alpha_{Lipid\text{-}Water}$ values vary significantly
130 for different species of eukaryotic algae grown under identical conditions (Schouten et
131 al., 2006; Zhang and Sachs, 2007; Chivall et al., 2014; M'Boule et al, 2014;
132 Heinzelmann et al., 2015).
133 Additionally, the trophic status of a lake could affect sedimentary δ^2H_{Lipid}
134 values by changing the sedimentary redox conditions and the activity of different types

of heterotrophic microbes. For example, Schwab et al. (2015) demonstrated that δ^2H values of dinosterol (4α,23,24-trimethyl-5α-cholest-22E-en3-ol) accumulating in surface sediments from seven stratified tropical lakes in Cameroon were enriched in ^2H relative to dinosterol in suspended particles, and that this enrichment was greater in more eutrophic lakes, as indicated by the redox potential of the oxic-anoxic interface. ^2H-enrichment of sedimentary dinosterol relative to that in the water column also increased with the ratio of dinostanol to dinosterol, suggesting that hydrogenation of sterols by anaerobic bacteria preferentially reduces molecules that are depleted in ^2H (Schwab et al., 2015).

Finally, heterotrophic microbes can produce some of the same compounds as photoautotrophs, in particular several short-chain fatty acids (Volkman et al., 1980; Heinzelmann et al., 2016). Since $\alpha_{Lipid\text{-}Water}$ values can differ by as much as 0.500 depending on microbial metabolism (Li et al., 2009; X. Zhang et al, 2009; Osburn et al., 2011; Heinzelmann et al., 2015; Osburn et al., 2016), conditions that favor more input of fatty acids or other compounds from heterotrophs could also have a significant effect on the net δ^2H values of fatty acids in sediments. Increased sedimentary contributions of dinosterol from heterotrophic dinoflagellates are thus an alternative explanation for the ^2H-enrichment of dinosterol in the sediments of more eutrophic lakes in Cameroon (Schwab et al., 2015).

In order to evaluate the overall effect of lake trophic status on the δ^2H values of sedimentary lipids, we analyzed *n*-alkanoic acids, *n*-alkanols, phytol, and brassicasterol from core tops (0-1 cm) and sediment traps from ten lakes with different trophic states in central Switzerland. In addition to evaluating whether $\alpha_{Lipid\text{-}Water}$ values for each lipid varied with trophic status, we calculated the relative offset between lipids produced by different biosynthetic pathways and compared this to lake trophic state. Finally, in order to assess isotopic differences between freshly produced material and lipids accumulating in sediment, we determined fractionation factors between sediment trap and core top samples.

2. Methods

2.1 Site description and sample collection

Samples were collected in the spring of 2015 from ten lakes in central Switzerland with a large range of sizes and catchment areas (Figure 1; Table 1). The lakes were selected to span oligotrophic to hypereutrophic conditions, with recent depth-integrated, wintertime maximum total phosphorus concentrations spanning 3 – 102 µg/L (Table 1).

In lakes where the total depth exceeded 20 m, samples were collected with a Niskin bottle for water isotope and nutrient analyses from depths of 0, 5, 10, 15, and 20 m. In shallower lakes up to four such samples were collected at evenly spaced intervals. Isotope water samples were stored in airtight glass screw-cap vials, sealed with electrical tape, and stored at room temperature until analysis. Nutrient samples were stored in opaque bottles at 4 °C until analysis. Additional surface water isotope samples from all lakes were collected from 2 – 4 locations near the lakeshore in August 2015. From Lakes Greifen and Lucerne water samples were also collected at four additional time points (Ladd et al., 2017).

Two identical sediment traps with an active surface area of 130 cm^2 and a height of 76 cm (model # Eawag-130) were deployed in each lake in early April 2015 (Table 1). Traps were placed at a depth of 20 m, except in lakes with a total depth shallower than 20 m, in which case the traps were positioned 1 - 2 m above the sediment-water interface. After ~ 4 weeks (Table 1) the traps were retrieved, decanted, and sediments were transferred to screw-cap jars and stored frozen at -20 °C until analysis.

Sediment cores were collected with a gravity corer from the deepest point of each lake on the same date that the sediment traps were either deployed or retrieved. Surface sediments were sectioned at 1 cm intervals and stored frozen at -20 °C prior to analysis. In Lake Brienz it was not possible to retrieve an undisturbed sediment-water interface. This lake was therefore excluded from the core top analyses.

2.2 Water isotopes

Water samples were filtered through a 25 mm syringe filter with a 0.45 µm polyethersulfone membrane to remove particulate material and were analyzed by cavity ring down spectroscopy (CRDS) (L-2120i Water Isotope Analyzer, Picarro, Santa Clara, CA, USA) at ETH-Zürich. Each sample was injected seven times in sequence, with the first four injections discarded to avoid memory effects. Three laboratory standards (δ^2H = -160.3, -75.6, and 8.1‰, $\delta^{18}O$ = 22.50, -10.62, and 0.95‰,

201 respectively) were injected at the beginning and end of each sequence, as well as after
202 every seven samples. These laboratory standards were used to reference sample
203 measurements to the VSMOW scale and to monitor for instrumental drift. The average
204 analytical precision was 0.4‰ for hydrogen and 0.06‰ for oxygen.
205 Surface water samples collected from sites around the lake shore in 2015 were
206 analyzed by Thermal Combustion/Elemental Analysis – Isotope Ratio Mass
207 Spectrometry (TC/EA-IRMS) at the University of Basel, following the same protocols
208 described previously (Ladd et al., 2015).
209
210 *2.3 Nutrient data*
211 Nutrient analyses were performed on a San++ Flow Injection Analyzer (Skaler,
212 Breda, the Netherlands), following standardized protocols (ISO 13395:1996 for nitrite
213 and nitrate; Boltz and Mellon, 1948 for phosphorus and phosphate). Because water
214 samples were collected at different time points and depths among lakes, we opted to
215 use historic nutrient data collected by the Swiss Federal Office of the Environment
216 (BAFU) and cantonal environmental offices to assess relationships between our
217 measurements and total phosphorus. Total phosphorus values used in this study
218 represent depth-integrated, winter maximum values from the three years prior to
219 sampling (BAFU; Bern Building, Traffic, and Energy Directorate; Lucerne
220 Environment and Energy) and are summarized in Table 1.
221
222 *2.4 Sediment accumulation rates*
223 Material from the upper portion of each core (upper 30 cm or upper 70 cm,
224 depending on expected accumulation rate) was analyzed using a high purity
225 Germanium Well Gamma Spectrometer (GCW3022-7500, Canberra, Meridian, CT,
226 USA). Accumulation rates were determined based on changes in unsupported ^{210}Pb
227 activity, which was calculated using measurements of ^{210}Pb and ^{226}Ra activities.
228 Accumulation rates were confirmed by two spikes in ^{137}Cs activity, which correspond
229 to maxima associated with the cessation of atmospheric nuclear weapons testing
230 (1963) and the Chernobyl nuclear meltdown (1986). Calculated sediment
231 accumulation rates are reported in Table 1, and ranged from 0.2 to 2 cm/year.
232
233 *2.5 Lipid extraction and purification*

A recovery standard including *n*-$C_{19:0}$ alkanoic acid and *n*-C_{19} alkanol was quantitatively added to freeze-dried, homogenized sediment, directly prior to extraction in 20 mL of 9:1 Dichloromethane/Methanol (DCM/MeOH) in a Microwave Reaction System (SolvPro, Anton Paar, Graz, Austria), following protocols modified from those of Kornilova and Rosell-Mele (2003). The microwave was heated to 70 °C over two minutes and held at 70 °C for 5 minutes. The resulting total lipid extract was evaporated to dryness under a gentle stream of nitrogen and saponified in 3:2 1N KOH in MeOH and DCM-extracted nanopure water at 70 °C for three hours. Neutral compounds were extracted with hexane, the remaining aqueous phase was acidified to pH < 2, and the fatty acids were then extracted with hexane. The fatty acid fraction was methylated to produce fatty acid methyl esters (FAMEs) using 1 mL of BF_3 in MeOH (14% by volume, Sigma Aldrich) for 2 hours at 100 °C. After adding 2 mL of DCM-extracted nanopure water, the FAMEs were extracted using hexane.

Neutral fractions were further separated into compound classes using Si gel column chromatography. The neutral fraction was dissolved in hexane and loaded onto a 500 mg/6 mL pre-packed Si column (Biotage, Uppsala, Sweden). Hydrocarbons eluted with 4 mL of hexane, ketones with 4 mL of 2:1 hexane/DCM, alcohols with 4 mL 19:1 DCM/MeOH, and remaining polar compounds with 4 mL of MeOH. The alcohol fraction was acetylated by dissolving in 50 μL of 1:1 acetic anhydride and pyridine and heating at 70 °C for 30 minutes. The acetylated alcohol fractions were subsequently dissolved in 4:1 hexane/DCM and loaded onto a 6 mL column containing 0.5 g of solvent rinsed Si gel impregnated with $AgNO_3$ (10% by weight, Sigma Aldrich). Phytol and *n*-alkanols eluted in the first fraction with 20 mL of 4:1 hexane/DCM, a second fraction containing non-target compounds was eluted with 20 mL of 1:1 hexane/DCM, and a third fraction containing brassicasterol was eluted with 16 mL of DCM.

Purified samples were quantified by gas chromatography with a flame ionization detector (GC-FID) (GC-2010 Plus, Shimadzu, Japan). An AOC-20i autosampler (Shimadzu) injected samples through a split/splitless injector operated in splitless mode at 280 °C. Samples were injected onto an InertCap 5MS/NP column (0.25 mm x 30 m x 0.25 μm, GL Sciences, Japan), which was heated from 70 °C to 130 °C at 20 °C/min, then to 320 °C at 4 °C/min, and held at 320 °C for 20 minutes. All fractions were quantified relative to recovery standards of *n*-$C_{19:0}$ fatty acid and *n*-C_{19} alkanol. Samples were identified by comparing their retention times to those of

laboratory standards, and by analyzing them under identical chromatographic conditions by gas chromatography – mass spectrometry (GC-MS) with a QP2020 mass spectrometer (Shimadzu, Japan) and comparing the resulting mass spectra to published mass spectra.

2.6 Lipid δ^2H measurements

Compound specific δ^2H values were obtained using gas chromatography – isotope ratio mass spectrometry (GC-IRMS). Samples were injected with a TriPlusRSH autosampler to a PTV inlet operated in splitless mode at 280 °C on a GC-1310 gas chromatograph (Thermo Scientific, Bremen, Germany) equipped with an InertCap 5MS/NP column (0.25 mm x 30 m x 0.25 μm) (GL Sciences, Japan) and interfaced to a Delta V Advantage IRMS (Thermo Scientific) with a ConFlow IV (Thermo Scientific). The GC oven was heated from 80 °C to 215 °C at 15 °C/min, then to 320 °C at 5 °C/min, and held at 320 °C for 10 minutes. Column effluent was pyrolyzed at 1420 °C.

Isotope values were measured using Thermo Isodat 3.0 software relative to pulses of working gas measured at the beginning and end of each analysis. Sample δ^2H values were normalized to the VSMOW scale using the slope and intercept of measured and known values of isotopic standards (*n*-$C_{17, 19, 21, 23, 25, 28,}$ and $_{34}$ alkanes, Arndt Schimmelmann, Indiana University), which were run at the beginning and end of each sequence, as well as after every 6 to 8 sample injections. Offsets between measured and known values for these standards were used to correct for any drift over the course of the sequence or any isotope effects associated with peak area or retention time. The standard deviation for these standards averaged 4‰ and the average offset from their known values was 1‰.

An additional quality control sample of *n*-C_{29} alkane was measured three times in each sequence, and the δ^2H value was -139 ± 5‰ (n = 42) over the period of analysis. The H_3^+ factor was measured at the beginning of each sequence and averaged 3.6 ± 0.3 ppm nA^{-1} during the analysis period (Sessions et al., 2001). Samples were corrected for hydrogen added during derivatization using isotopic mass balance. The δ^2H composition of the hydrogen added during methylation was determined by methylating phthalic acid of known isotopic composition (provided by A.

Schimmelmann, U. Indiana). The δ^2H values of the added acetyl group were determined by analyzing acetylated and unacetylated *n*-C_{10} alkanol.

3. Results

3.1 Water δ^2H values

Lake water δ^2H values ranged from -94 ± 1‰ in Lake Brienz to -57 ± 2‰ in Lake Soppen, while lake water $\delta^{18}O$ values ranged from -12.6 ± 0.2‰ in Lake Thun to -7.4 ± 0.2‰ in Lake Soppen (Table 1). In general, the lowest water isotope values were found in large lakes closer to the Alps that are fed by rivers draining high elevation alpine catchments, such as Lakes Brienz, Thun, and Lucerne. Sites with the highest water isotope values were relatively small lakes in the northern part of the study area, such as Lakes Soppen, Inkwil, and Mauen (Table 1).

Lake water isotope values varied little with depth, with an average standard deviation of 0.9‰ for hydrogen and 0.1‰ for oxygen for the samples collected at different depths within each individual water profile (n = 20). Likewise, there were only small changes in water isotopes between the date when the sediment traps were deployed and when they were retrieved, with differences averaging 2‰ for hydrogen and 0.2‰ for oxygen (Table 1). In Lakes Greifen and Lucerne water samples were collected and analyzed at monthly intervals from April to September 2015, with δ^2H values varying by no more than 6‰ and $\delta^{18}O$ values by no more than 1.8‰ (Ladd et al., 2017). Additional surface water samples collected from near shore sites in all ten lakes in August 2015 also had δ^2H and $\delta^{18}O$ values that were consistent with those measured from the springtime water column samples, with the exception of Lake Inkwil, the smallest lake in the study, where water isotope values were enriched by ~12‰ in August (Table 1).

3.2 Lipid concentrations

Lipid concentrations in sediment traps and surface sediments were determined for 25 fatty acids (*n*-$C_{14:0}$ through *n*-$C_{30:0}$ alkanonic acids, and several common unsaturated compounds among those chain lengths) (Table S1). On average, *n*-$C_{16:0}$ (palmitic acid) was the most common fatty acid, with core top concentrations ranging from 3.4 µg/g dry sediment (d. s.) in Lake Thun to 136 µg/g d.s. in Lake Rot (Table

S1). Concentrations of individual fatty acids were typically 1-2 orders of magnitude higher in the sediment trap samples, where *n*-$C_{16:0}$ concentrations ranged from 32 μg/g d.s. in Lake Sarnen to 2,477 μg/g d.s. in Lake Inkwil (Table S1).

The alcohol fraction was characterized by phytol, *n*-alkanols (*n*-$C_{16\text{-ol}}$ to *n*-$C_{26\text{-ol}}$), and sterols, of which β-sitosterol, brassicasterol, cholesterol, and stigmasterol were the most common (concentrations and systematic names provided in Table S1). In most samples, phytol was the most abundant alcohol, with concentrations in the core tops ranging from 1.4 μg/g d.s. (Lake Thun) to 212 μg/g d.s. (Lake Rot). Phytol concentrations in the sediment traps ranged from 1.8 μg/g d.s. (Lake Brienz) to 833 μg/g d.s. (Lake Soppen) (Table S1). 5α-cholestanol was common in the core top samples, but generally absent or only present in trace amounts in the sediment traps (Table S1). Although concentrations of most alcohols were lower in core tops than in the corresponding sediment traps, the differences were typically smaller than those observed for fatty acids (Table S1).

3.3 Compound specific lipid δ^2H values

Given the range in δ^2H_{Water} values among lakes (Table 1), $\alpha_{Lipid\text{-}Water}$ values, which represent the offset between δ^2H_{Water} values and δ^2H_{Lipid} values (reported in Tables S2 and S3), are generally more useful for comparisons among lakes than δ^2H_{Lipid} values. The lowest $\alpha_{Lipid\text{-}Water}$ values were observed for phytol, which had a mean value of 0.674 ± 0.015 (1σ) in the core tops and ranged from 0.645 ± 0.10 in Lake Greifen to 0.690 ± 0.010 in Lake Inkwil (Table 2). Mean $\alpha_{Phytol\text{-}Water}$ values in the sediment traps were 0.660 ± 0.016, and ranged from 0.636 ± 0.002 in Lake Lucerne to 0.689 ± 0.006 in Lake Soppen (Table 3). Brassicasterol $\alpha_{Lipid\text{-}Water}$ values were higher than those of phytol, with a mean value of 0.776 ± 0.026 in the core tops, where $\alpha_{Brassicasterol\text{-}Water}$ values ranged from 0.746 ± 0.004 (Lake Greifen) to 0.822 ± 0.007 (Lake Thun) (Table 2). For the sediment traps, the mean $\alpha_{Brassicasterol\text{-}Water}$ value was 0.779 ± 0.024, the lowest value was in Lake Soppen (0.741 ± 0.003), and the highest value was in Lake Thun (0.807 ± 0.003) (Table 3).

Acetogenic lipids, including *n*-alkanols (*n*-C_{14} to *n*-C_{26}) and *n*-alkanoic acids (*n*-C_{14} to *n*C_{30}), were generally more enriched than the isoprenoids phytol and brassicasterol (Tables S2 and S3), and correspondingly had higher $\alpha_{Lipid\text{-}Water}$ values (Tables 2 and 3). For *n*-alkanols, the mean $\alpha_{Lipid\text{-}Water}$ value in the core tops was 0.876 ±

0.022 and the mean value in the sediment traps was 0.870 ± 0.028. The lowest *n*-alkanol $\alpha_{Lipid\text{-}Water}$ value was associated with *n*-C_{26} alkanol in the Lake Baldegg core top (0.814 ± 0.002), while the highest was from *n*-C_{16} alkanol in the Lake Inkwil core top (0.938 ± 0.006) (Table 2). For *n*-alkanoic acids, the mean $\alpha_{Lipid\text{-}Water}$ value in the core tops was 0.880 ± 0.030 and the mean value in the sediment traps was 0.828 ± 0.028. The lowest $\alpha_{Lipid\text{-}Water}$ value for an *n*-alkanoic acid was *n*-$C_{18:3\omega3}$ in the sediment traps from Lake Greifen (0.781 ± 0.001), and the highest was for *n*-$C_{30:0}$ from the Lake Lucerne core top (0.924 ± 0.003) (Tables 2 and 3). The concentrations of sediment trap *n*-alkanoic acids with C > 18 were typically 1-2 orders of magnitude lower than those of $C_{14\text{-}18}$ (Table S1), and these samples were only analyzed at concentrations suitable for determining δ^2H values of the shorter chain lengths.

In most cases, lipid δ^2H values were not significantly correlated with lake water δ^2H values (Fig. 2). Notable exceptions were phytol, with δ^2H values in sediment traps that were significantly correlated with lake water δ^2H values ($R^2 = 0.69$, $p = 0.003$) (Fig. 2 and 3), sediment trap δ^2H values of *n*-$C_{16:0}$ alkanoic acids ($R^2 = 0.42$, $p = 0.04$), and core top *n*-$C_{28:0}$ alkanoic acids ($R^2 = 0.86$, $p = 0.0009$) (Fig. 2 and 3). Sediment trap *n*-C_{26} alkanol δ^2H values were negatively correlated with those of lake water ($R^2 = 0.69$; $p = 0.003$) (Fig. 2). Weaker correlations that were not significant at the 95% confidence level were observed to be positive for most lipids (13 out of 19 compounds measured in core tops and 8 out of 14 compounds measured in sediment traps) (Fig. 2).

3.4 Relationships between $\alpha_{Lipid\text{-}Water}$ and trophic state

For most compounds, the fractionation factor between the lipid and lake water δ^2H values, $\alpha_{Lipid\text{-}Water}$, was not significantly correlated with the depth-integrated total phosphorus concentrations of lake water (Fig. 4). When significant correlations did exist, they were almost always negative. This was the case for brassicasterol, *n*-$C_{16:0}$ alkanoic acid, and *n*-$C_{18:1}$ alkanoic acid in the core tops, and for *n*-C_{24} alkanol, *n*-C_{26} alkanol, brassicasterol, and *n*-$C_{18:1}$ alkanoic acid in the sediment traps (Fig. 4 and 5). Since the lipids were in all cases depleted relative to the lake water, decreasing $\alpha_{Lipid\text{-}Water}$ values correspond to more ^2H-fractionation. The one exception was phytol in the sediment traps, for which $\alpha_{Lipid\text{-}Water}$ was significantly positively correlated with total phosphorus ($R^2 = 0.56$; $p = 0.01$) (Fig. 4 and 5).

399 *3.5 Fractionation between sediment trap and core top δ^2H values of individual lipids*

400 For the twelve compounds where it was possible to measure δ^2H values both in
401 the core top and in the sediment traps, the average fractionation factor between the two
402 values, $\alpha_{CoreTop\text{-}SedTrap}$ was statistically different from 1.000 (no fractionation) for only
403 four compounds: *n*-$C_{14:0}$, *n*-$C_{16:0}$, *n*-$C_{16:1\omega9}$, and *n*-$C_{18:0}$ alkanoic acids (Fig. 6a). For all
404 of these compounds, average $\alpha_{CoreTop\text{-}SedTrap}$ values were greater than 1.000, as core top
405 δ^2H values were enriched relative to those in the sediment traps (Fig. 6a). This
406 enrichment was greatest for compounds with core top concentrations that were less
407 than 10% of the concentration of those same compounds in the sediment trap samples
408 (Fig. 6b). For these compounds, $\alpha_{CoreTop\text{-}SedTrap}$ values averaged 1.032 ± 0.032 (Fig. 6b).
409 For compounds with core top concentrations between 10% and 100% of their sediment
410 trap concentrations, $\alpha_{CoreTop\text{-}SedTrap}$ values averaged 1.012 ± 0.024, and for compounds
411 with core top concentrations greater than or equal to those in the sediment traps,
412 $\alpha_{CoreTop\text{-}SedTrap}$ values averaged 1.010 ± 0.027 (Fig. 6b).
413
414 **4. Discussion**
415
416 *4.1 Relationship between δ^2H_{Lipid} values and δ^2H_{Water} values*

417 If water isotopes were the primary control on δ^2H_{Lipid} values in these lakes, one
418 would expect δ^2H_{Lipid} values to be positively correlated with δ^2H_{Water} values, and such
419 positive correlations did exist in the majority of cases (21 out of 32) (Fig. 2). However,
420 these positive correlations were significant in only three instances (Fig. 2). In the
421 sediment trap samples, δ^2H values of phytol and *n*-$C_{16:0}$ alkanoic acid, both of which
422 are produced by virtually all phytoplankton, were significantly positively correlated
423 with those of water (Fig. 2 and 3). This result suggests that relatively recently produced
424 compounds with a strong photoautotrophic aquatic source can reflect the δ^2H
425 composition of lake water and that net community fractionation averages out variations
426 in $\alpha_{Lipid\text{-}Water}$ among different sources. However, this signal is largely lost in the core
427 tops of these lakes, where neither phytol nor *n*-$C_{16:0}$ alkanoic acid δ^2H values were
428 significantly correlated with δ^2H_{Water} values (Fig. 2 and 3).

429 In the core tops, the only compound with δ^2H values that were significantly
430 correlated with δ^2H_{Water} values was *n*-$C_{28:0}$ alkanoic acid (Fig. 2). This result is
431 somewhat surprising, since this compound is typically presumed to derive from plant

waxes and therefore would not necessarily be expected to have δ^2H values that correlate with those of lake water. One possibility is that in these settings, the main source of *n*-$C_{28:0}$ alkanoic acid is indeed from aquatic organisms, as in some cases it is produced by microalgae (Volkman et al., 1980). A microalgal source of *n*-C_{28} alkanoic acid is unlikely in these lakes, however, given the distribution of fatty acids in the sediment traps. The fatty acids in the sediment traps were dominated by the *n*-C_{14} to *n*-C_{18} alkanoic acids, compounds which are typically associated with phytoplankton, and had proportionately less *n*-$C_{28:0}$ alkanoic acid than in the core top samples (Table S1). This pattern suggests that the sediment trap samples primarily consisted of fresh microalgal material, which was not abundant in *n*-$C_{28:0}$ alkanoic acid.

A more likely possibility for the positive correlation between lake water and *n*-$C_{28:0}$ alkanoic acid δ^2H values is that the lakes closest to the Alps, which tend to have the most ^2H-depleted water isotopes and *n*-$C_{28:0}$ fatty acids, could contain significantly more plant waxes derived from high elevation vegetation relative to locally sourced low-elevation plant material. Notably, δ^2H values *n*-$C_{30:0}$ fatty acids, which are also commonly considered to be leaf wax constituents of higher plants (Meyers and Ishiwatari, 1993), do not co-vary with those of *n*-$C_{28:0}$ or of lake water (Figure 2). This suggests that different groups of plants are the primary sources of these two molecules in central Swiss lake sediments, which is consistent with previous studies that indicate that fatty acid distributions and H-isotope fractionation are not consistent among higher plant taxa (Diefendorf et al., 2011; Gao et al., 2014; Feakins et al, 2016).

For all other compounds, a significant positive correlation between δ^2H_{Lipid} and δ^2H_{Water} was not observed, although $\delta^2H_{n\text{-}C26\text{-}ol}$ is strongly negatively correlated with δ^2H_{Water} in the sediment trap samples (Fig. 2). This indicates that other variables exert stronger controls on δ^2H_{Lipid} values than δ^2H_{Water} values in central Swiss lakes. Although previous core top calibrations spanning larger geographical areas have typically shown good agreement between δ^2H_{Water} and δ^2H_{Lipid} (Sauer et al., 2001; Huang et al., 2004; Sachse et al., 2004; Hou et al, 2008), the large variability we observe in $\alpha_{Lipid\text{-}Water}$ values among lakes in a relatively small area (Tables 2 and 3) suggests that δ^2H_{Lipid} values are not always indicative of δ^2H_{Water}. This relationship may be especially vulnerable in locations where lake trophic status varies significantly, and among low-elevation lakes with differing proximity to high-elevation catchments. As catchment shape is unlikely to change significantly on the centennial to millennial timescales upon which down core δ^2H_{Lipid} values are typically applied to reconstruct

hydrologic change, this may not hinder the ability to reconstruct changes in source water isotopes within a single water body over time. On the other hand, changes in trophic status may complicate the hydrologic signal recorded by lipids. In settings where phytoplankton growth conditions may have changed significantly, we recommend that δ^2H_{Lipid} values should only be interpreted as δ^2H_{Water} proxies if supported by other lines of sedimentary evidence, one of which may be changes in the relative offsets among δ^2H values from different classes of lipids, as explored below.

4.2 Potential causes of variability in $\alpha_{Lipid\text{-}Water}$ values

Although δ^2H_{Lipid} values in the studied lakes were often poorly correlated with δ^2H_{Water} values (Fig. 2, Section 4.1), there was nevertheless wide variability in δ^2H_{Lipid} values among and within compounds (Tables S2 and S3), which may contain useful information. Variability in δ^2H_{Lipid} values may reflect changes in net $\alpha_{Lipid\text{-}Water}$ values during lipid synthesis by a single taxonomic group. Alternatively, they may be primarily due to changes in the relative contributions from different sources. These two possibilities are explored below.

4.2.1 Potential influence of phytoplankton productivity on δ^2H_{Lipid} values

One potential source of variability in δ^2H_{Lipid} values is variations in $\alpha_{Lipid\text{-}Water}$ related to nutrient availability (Z. Zhang et al., 2009; Sachs and Kawka, 2015). Laboratory cultures of marine eukaryotic algae indicate that increased growth rates and higher nutrient availability can result in more ^2H-fractionation (lower $\alpha_{Lipid\text{-}Water}$) values for sterols, alkenones, and in some cases *n*-alkanoic acids (Schouten et al., 2006; Z. Zhang et al., 2009; Sachs and Kawka, 2015). In lakes with higher total phosphorus concentrations, $\alpha_{Brassicasterol\text{-}Water}$ values were significantly lower in both core top and sediment trap samples (Fig. 4 and 5), which is consistent with these laboratory results. Sachs and Kawka (2015) suggested that decreasing $\alpha_{Lipid\text{-}Water}$ values for sterols at higher growth rates could be explained by a greater proportion of the H incorporated into sterols being derived from extremely ^2H-depleted NADPH in photosystem I at the expense of relatively ^2H-enriched NADPH from the oxidative pentose phosphate pathway.

In contrast to the $\alpha_{Brassicasterol\text{-}Water}$ values, $\alpha_{Phytol\text{-}Water}$ values increased with total phosphorus, indicating less net fractionation (Fig. 5). No laboratory growth rate studies

have reported δ^2H_{Phytol} values, so it is unknown if a similar positive relationship between $\alpha_{Phytol\text{-}Water}$ values and growth rate exists in cultures. However, if this is a robust finding, it suggests that fundamentally different processes are responsible for changes in $\alpha_{Phytol\text{-}Water}$ with nutrient availability than those previously proposed for changes in $\alpha_{Sterol\text{-}Water}$. Intriguingly, similar opposing trends in $\alpha_{Sterol\text{-}Water}$ and $\alpha_{Phytol\text{-}Water}$ were observed as light levels increased in a recent study with the marine diatom *Thalassiosira pseudonana* grown in chemostats (Sachs et al., 2017). It is therefore possible that the same underlying biochemical mechanisms are responsible for changes in H isotope fractionation under low-light and low-phosphorus conditions, which is not unreasonable since a lack of either light or nutrients inhibits photosynthesis, and since low phosphorus availability causes relatively more carbon fixation to occur in the dark (Morris et al., 1971; Theodorou et al., 1991).

Different H isotope responses to the same environmental gradient could be due to the different biosynthetic pathways used to produce each type of compound. Sterols are commonly produced by the mevalonate (MVA) pathway in the cytosol (Vranová et al., 2012), although they can also be produced by the 2-*C*-methyl-D-erythritol 4-phosphate/1-deoxy-D-xylulose 5-phosphate (MEP-DOXP) pathway (Eisenreich et al., 2004; Miller et al., 2012; Vranová et al., 2012). Interestingly, for green algae, the MEP-DOXP pathway is the only means of sterol production, since this group lacks the MVA mechanism entirely (Miller et al., 2012). Phytol, on the other hand, is produced exclusively in the plastid via the DOXP pathway (Lichtenthaler, 1999). The most plausible source of diverging $\alpha_{Lipid\text{-}Water}$ values for sterols and phytol are therefore downstream of the branch point between the MVA and DOXP pathways, and are not related to whole cell processes such as intracellular water or the initial incorporation of H into carbohydrates. Exact mechanisms for diverging $\alpha_{Phytol\text{-}Water}$ and $\alpha_{Sterol\text{-}Water}$ values, which could include up regulation of sterol production by the MEP-DOXP pathway and more pyruvate production through glycolysis in the cytosol at high nutrient concentrations (Z. Zhang et al., 2009; Sachs and Kawka, 2015; Sachs et al., 2017), cannot be assessed with our data set. This observation could be further explored through culturing studies that combine lipid isotopes and transcriptomic data, and potentially developed as an indicator of phytoplankton growth conditions.

Such an indicator of growth conditions would be best described through the relative offset between the two lipids, which, although they are not a direct substrate-product pair, can be expressed as $\varepsilon_{Lipid\ 1\text{-}Lipid\ 2}$ values (where $\varepsilon_{Lipid\ 1\text{-}Lipid\ 2} = [((\delta^2H_{Lipid\ 1} +$

1000)/ ($\delta^2H_{Lipid\ 2}$ + 1000)) -1] * 1000). Due to the non-linear scaling of δ notation, and the wide natural variability in δ^2H values, ε values are more appropriate for comparing δ^2H values than Δ values ($\Delta = \delta^2H_{Lipid\ 1} - \delta^2H_{Lipid\ 2}$), and have the advantage of being independent of source water δ^2H values. Smaller offsets between phytol and sterol δ^2H values (smaller $\varepsilon_{Sterol\text{-}Phytol}$ values) were observed as conditions increasingly favored photosynthesis (increased phosphorus or increased light) (Fig. 7; Table 4). Additionally, similar trends were observed for the ^2H-offsets between *n*-$C_{16:0}$ fatty acid and both phytol and sterol values for the lake samples and the chemostats (Fig. 7), despite uncertainty about the sources of *n*-$C_{16:0}$ fatty acid in the lakes (section 4.2.2). These patterns suggest that similar biochemical mechanisms may underlie changes in the ^2H-offset between fatty acids and both types of isoprenoids under high nutrient and high light conditions, and that smaller $\varepsilon_{Sterol\text{-}Phytol}$ values correspond to more favorable growth conditions, while larger $\varepsilon_{Sterol\text{-}Phytol}$ values indicate greater environmental stress. Such an indicator could be helpful for distinguishing when down core changes in δ^2H_{Lipid} values are likely to represent a change in growth conditions (changing $\varepsilon_{Sterol\text{-}Phytol}$ values) and when they are primarily a hydrological signal (changing δ^2H_{Lipid} values without a concurrent change in $\varepsilon_{Sterol\text{-}Phytol}$ values). Furthermore, it might be possible to apply $\varepsilon_{Sterol\text{-}Phytol}$ values to δ^2H values from a single compound to remove the growth effect and to recover the underlying hydrologic signal. Likewise, $\varepsilon_{Sterol\text{-}Phytol}$ values could provide a useful constraint on existing phytoplankton lipid-based proxies (such as $U^{K'}_{37}$ for temperature or $\delta^{13}C$ values of alkenones for pCO_2), which can also be sensitive to growth conditions.

4.2.2 Potential influence of lipid source on δ^2H_{Lipid} values

Much of the variability in δ^2H_{Lipid} values observed for the same molecule among different lakes could be due to varying contributions from different sources. The hydrogen isotope effect of variable sources is expected to be largest for compounds that can be produced by heterotrophic and chemoautotrophic organisms as well as photoautotrophs (X. Zhang et al., 2009; Osburn et al., 2011; Heinzelmann et al., 2015). Hydrogen isotope fractionation associated with short-chain fatty acid biosynthesis can vary by several hundred ‰ among organisms with different core metabolisms, with fatty acids produced by heterotrophs being enriched in ^2H by as much as 500‰ relative to photoautotrophs and chemoautotrophs growing under

identical temperature, light, and growth water conditions (X. Zhang et al., 2009; Heinzelmann et al., 2015). Heterotrophic contributions can be expected to influence the δ^2H values of ubiquitous short-chain fatty acids such as *n*-$C_{16:0}$ and *n*-$C_{18:1}$ fatty acids. Although these compounds constitute a large portion of the total lipid extract from many phytoplankton, they can also be produced in significant quantities by heterotrophs and chemoautotrophs (summarized by Heinzelmann et al., 2016). Likewise, short and mid-chain *n*-alkanols can be produced by phytoplankton, including as the side-chain in cyanobacterial glycolipids (Sinninghe Damsté et al., 2001; Castañeda and Schouten, 2011; Nelson and Sachs, 2016), but are also produced by zooplankton (Sargent et al., 1977; Pearson et al., 2001). Changes in the relative contributions from each of these sources can have profound effects on the composite δ^2H_{Lipid} values accumulating in sediment, and may explain why in most cases these values were not significantly correlated with δ^2H_{Water} (Fig. 2).

Even for compounds that are specific to photoautotrophic sources, such as phytol and brassicasterol, changing contributions from different sources could contribute to some of the variability in δ^2H_{Lipid} values. As the side-chain from chlorophyll *a*, *b*, *d*, and *f*, phytol is a common constituent of non-aquatic plants, which have different source water than phytoplankton and are therefore expected to have different δ^2H values. However, most phytol accumulating in lake sediments is considered to have an aquatic source, since chlorophyll and phytol rapidly degrade in light and oxic environments, and it is difficult to transport and preserve terrestrial phytol in lacustrine sediments (Meyers and Takeuchi, 1981). Low concentrations of phytol in sediment traps and core tops from low productivity lakes (Table S1) support the assumption that most phytol in Swiss lake sediments is aquatically sourced. Likewise, brassicasterol is primarily derived from eukaryotic algae in aquatic sediments (Volkman et al., 2003) although it has in some instances been observed in plant oils (Zarrouk et al., 2009). Even if phytol and brassicasterol are limited to phytoplankton sources, changes in the algal community composition could affect their aggregate δ^2H values, as different $\alpha_{Lipid\text{-}Water}$ values have been observed for alkenones and fatty acids produced by different species of eukaryotic algae grown in batch cultures under identical conditions (Schouten et al., 2006; Zhang and Sachs, 2007; M'Boule et al., 2014; Chivall et al., 2014; Heinzelmann et al., 2015). The distributions of phytoplankton taxa can co-vary with increasing eutrophication and with the re-oligotrophication of previously eutrophic lakes, which has occurred in many of the

600 larger lakes in Switzerland (Pomati et al., 2011; Monchamp et al., 2018). While no
601 studies to date have investigated variability in $\alpha_{Lipid\text{-}Water}$ values among freshwater
602 diatoms or other known brassicasterol producers, it is possible that the brassicasterol
603 producers that thrive in oligotrophic systems have inherently higher $\alpha_{Lipid\text{-}Water}$ values
604 than brassicasterol producers that are abundant in more eutrophic lakes. If this is the
605 case, it would result in the negative correlations observed between $\alpha_{Brassicasterol\text{-}Water}$
606 values and total P (Fig. 5), and could suggest that no changes in $\alpha_{Brassicasterol\text{-}Water}$ within
607 a single species are necessary to explain this relationship. Laboratory investigations of
608 $\alpha_{Brassicasterol\text{-}Water}$ values among freshwater producers would help determine whether
609 community composition is a likely source of variability in $\alpha_{Brassicasterol\text{-}Water}$ in natural
610 settings.
611
612 *4.3 Differences between sediment trap and core top δ^2H_{Lipid} values*
613 Core top δ^2H values were enriched in ^{2}H relative to those in the sediment traps
614 for all compounds in which the average $\alpha_{CoreTop\text{-}SedTrap}$ values were significantly
615 different than 1.000 (Fig. 6). This relationship was observed for most short-chain *n*-
616 alkanoic acids and could be explained in three ways: (i) seasonal bias due to the longer
617 time interval integrated into the core top, (ii) heterotrophic production of short-chain
618 fatty acids in the surface sediment, or (iii) microbial degradation of *n*-alkanoic acids in
619 the water column and/or surface sediment.
620 Seasonal bias is unlikely to account for the relatively enriched δ^2H values of
621 the core top *n*-alkanoic acids, as the δ^2H values of short-chain acids collected from
622 filter samples in suspended particles in the surface waters of Lakes Greifen and
623 Lucerne decrease from spring to summer by as much as 150‰ (Ladd et al., 2017). The
624 sediment traps were in place in April and May, when surface water *n*-alkanoic δ^2H
625 values were most enriched. Therefore, one would expect the compounds in the core
626 tops, which integrate over the whole year for multiple annual cycles, to be more
627 depleted in ^{2}H than those in the sediment traps if the difference between the two were
628 exclusively due to a seasonality effect. Additionally, the flux of organic matter to the
629 sediments is expected to be highest during the autumn in these lakes (Hollander et al.,
630 1992; Lotter et al., 1997; Teranes et al., 1999), which should, if anything, bias the core
631 top signal towards even more ^{2}H-depleted values than the sediment traps, since newly

632 produced fatty acids in the suspended organic matter are ^{2}H-depleted in autumn
633 relative to spring (Ladd et al., 2017).
634 A second possible explanation for ^{2}H-enrichment of core-top fatty acids could
635 be increased heterotrophic inputs of these compounds relative to in the sediment traps.
636 As described in section 4.2.2, heterotrophic microbes produce fatty acids that can be
637 enriched in ^{2}H by several hundred ‰ relative to those produced by photoautotrophs
638 grown in the same water (X. Zhang et al. 2009; Heinzelmann et al., 2015). Additional
639 heterotrophic contributions of generic compounds that can be produced by both
640 photoautotrophs and heterotrophs would therefore be expected to result in increased
641 δ^{2}H values. Such ^{2}H-enrichment was indeed observed for ubiquitous fatty acids in
642 settings with greater probable heterotrophic contributions in Santa Barbara Basin
643 sediments (Li et al., 2009). In contrast to the Santa Barbara Basin sediments, elevated
644 $\alpha_{CoreTop\text{-}SedTrap}$ values for generic fatty acids were not accompanied by an increase in the
645 abundance of bacterial biomarkers, such as *n*-$C_{15:1}$ and *n*-$C_{17:1}$ fatty acids (Table S1).
646 Although it is not the case that all *n*-$C_{16:0}$ producing bacteria also produce *n*-$C_{15:1}$ and
647 *n*-$C_{17:1}$ fatty acids (Heinzelmann et al., 2016), the low abundance of these bacterial
648 biomarkers also does not support a large bacterial contribution of generic fatty acids.
649 Additionally, since generic fatty acid concentrations declined precipitously between
650 the sediment traps and the core tops (Table S1), it is unlikely that there is a large
651 sedimentary source of these compounds, at least in the surface sediment.
652 Rather, the most plausible explanation for ^{2}H-enrichment of fatty acids in the core tops
653 relative to the sediment traps is that the majority of these compounds were degraded in
654 the water column prior to reaching the surface sediment. Sterols in core top samples
655 collected in estuaries and lakes have been observed to be ^{2}H-enriched relative to those
656 in overlying suspended particles (Sachs and Schwab, 2011; Schwab et al., 2015),
657 which has been attributed to preferential degradation of the lighter isotopologues of
658 these compounds (Schwab et al., 2015). Likewise, *n*-alkanes that showed evidence of
659 microbial degradation due to improper laboratory storage conditions were ^{2}H-enriched
660 relative to freshly collected samples from the same site (Brittingham et al., 2017).
661 Although these studies do not conclusively demonstrate that microbial degradation will
662 result in ^{2}H-enrichment of the remaining *n*-alkanoic acids, it is consistent with the large
663 decrease *n*-alkanoic concentrations in the core tops relative to the sediment traps
664 (Table S1), and the fact that the greatest ^{2}H-enrichment was observed for compounds

665 whose concentrations decreased the most between the sediment traps and core tops
666 (Fig. 6b). The high potential for degradation of short-chain fatty acids in the water
667 column (Kawamura et al., 1987; Haddad et al., 1992; Ho and Meyers, 1994; Canuel
668 and Martens, 1996), and the likely isotopic impact of that degradation (Fig. 6b), would
669 thus caution against interpreting the down core δ^2H values of these compounds as a
670 water isotope signal.
671
672 **5. Conclusions**
673 In order to assess the influence of lake trophic status on the hydrogen isotope
674 composition of sedimentary lipid biomarkers, we analyzed sediment trap and core top
675 samples from ten lakes with different total phosphorus concentrations in central
676 Switzerland. For the majority of compounds, δ^2H_{Lipid} values were positively correlated
677 with δ^2H_{Water} values, but these relationships were weak and only significant in the case
678 of phytol and *n*-$C_{16:0}$ alkanoic acid in the sediment traps, and *n*-$C_{28:0}$ alkanoic acid in
679 the core tops. This result is problematic for the direct qualitative interpretation of down
680 core δ^2H_{Lipid} values as a signal of water isotopes in locations where eutrophication has
681 caused changes in the phytoplankton community structure, or where proximity to
682 mountains may bring lipids produced at high elevations to low elevation depocenters.
683 Further complicating the use of generic short-chain fatty acid δ^2H values is their
684 pattern of ^2H-enrichment in surface sediments relative to sediment traps. This ^2H-
685 enrichment may be due to variable contributions from heterotrophs in surface
686 sediments, but is more likely caused by isotopically selective degradation of fatty
687 acids.
688 Phytoplankton-specific sterols avoid some of the issues related to lipid source,
689 and have therefore been proposed as an attractive target for water isotope
690 reconstructions. However, our results indicate that hydrogen isotope fractionation
691 associated with these compounds is sensitive to changes in nutrient regime, either
692 because of changes in net $\alpha_{Lipid\text{-}Water}$ values during lipid synthesis by a single taxonomic
693 group, or due to changes in the relative contributions from different phytoplankton
694 taxa. In agreement with previous results from laboratory cultures, the fractionation
695 factor $\alpha_{Lipid\text{-}Water}$ decreased for brassicasterol, a sterol commonly associated with
696 diatoms, as total phosphorus concentrations increased in both the sediment traps (R^2 =
697 0.66) and core tops (R^2 = 0.66). In constrast, as $\alpha_{Lipid\text{-}Water}$ values decreased for

brassicasterol, they increased for phytol, the side-chain moiety of chlorophyll, resulting in phytol and brassicasterol δ^2H values that became increasingly similar to one another. By concurrently measuring δ^2H values of phytol and algal-derived sterols from the same sediment and calculating their relative offset from each other, it may be possible to determine when the δ^2H values changed because of variable fractionation (resulting in different $\varepsilon_{Sterol\text{-}Phytol}$ values), and when they are changed primarily because of a change in source water isotopes (indicated by relatively constant $\varepsilon_{Sterol\text{-}Phytol}$ values). A reanalysis of previously published data suggests that $\varepsilon_{Sterol\text{-}Phytol}$ values also decrease as light intensity increases. The similar response of $\varepsilon_{Sterol\text{-}Phytol}$ values to both increasing phosphorus and light suggests that $\varepsilon_{Sterol\text{-}Phytol}$ values may have potential as a proxy for past phytoplankton growth, with biochemical responses to conditions favoring photosynthesis and growth resulting in opposing changes in H isotope fractionation for these two types of isoprenoids. Our data demonstrate how comparing the differences between δ^2H values from multiple lipids in a sediment record can distinguish cases where variability in δ^2H values were driven by biochemical and/or ecological factors from those that reflect a primary hydroclimate signal.

Acknowledgements

This research was funded by a National Science Foundation Earth Sciences Postdoctoral Fellowship (Award #1452254) to NL and by Eawag internal funds. Alois Zwyssig and Alfred Lück assisted with sample collection. Serge Robert and Anton Hertler assisted with lipid sample preparation and laboratory analyses. Daniel Montluçon at ETH-Zurich measured the water isotopes from April and May, 2015. Ansgar Kahmen and Cristina Moreno Gutierrez from the University of Basel kindly shared water isotope data from August 2015. Robert Lovas (Luzern EWE) and Markus Zeh (Bern BVE) provided historical phosphorus data. We had productive conversations with Ashley Maloney, Julian Sachs, and Anita Narwani that improved the study design and interpretation of results. Three anonymous reviewers and associate editor Ann Pearson provided helpful comments that strengthened the final manuscript. We are grateful for all of their contributions.

Data Availability

The data set associated with this paper is available at https://doi.org/10.3929/ethz-b-000265859

Figure Captions

Figure 1: Map of Switzerland with the locations of targeted lakes. The background shading in the elevation map (panel a) shows elevation from the 30-arc second GTOPO30 digital elevation model from the United States Geological Survey. Total depth-integrated, wintertime maximum phosphorus concentrations for 2013-2015 are shown for sampled lakes (panel b). Water bodies shown in gray (panel b) were not sampled as part of this study. Lakes are numbered alphabetically and names and relevant characteristics of each are listed in Table 1.

Figure 2: R values of linear regressions of δ^2H_{Lipid} values relative to δ^2H_{Water} values for all analyzed compounds in core tops (blue circles) and sediment traps (pink squares). Filled symbols represent correlations that were significant at the 95% confidence level.

Figure 3: δ^2H_{Lipid} values plotted relative to δ^2H_{Water} values for *n*-$C_{16:0}$ alkanoic acid, brassicasterol, and phytol in sediment traps (panel a) and core tops (panel b). Shading represents 95% confidence intervals of linear regressions. Regression lines are only shown for significant correlations ($p < 0.05$).

Figure 4: R values of linear regressions of $\alpha_{Lipid\text{-}Water}$ values relative to total phosphorus concentrations for all analyzed compounds in core tops (blue circles) and sediment traps (pink squares). Filled symbols represent correlations that were significant at the 95% confidence level.

Figure 5: $\alpha_{Lipid\text{-}Water}$ values relative to total phosphorus for *n*-$C_{16:0}$ alkanoic acid, brassicasterol, and phytol in sediment traps (panel a) and core tops (panel b). Shading represents 95% confidence intervals of linear regressions. Regression lines are only shown for significant correlations ($p < 0.05$).

Figure 6: Fractionation factors between core top and sediment traps ($\alpha_{CoreTop\text{-}SedTrap}$) for all compounds that were abundant enough to measure in both sample sets. Box and whisker plots show means and distributions of $\alpha_{CoreTop\text{-}SedTrap}$ values from all lakes. Mean values that are significantly different from 1.000 (no fractionation) are indicated by *. Distributions are shown for individual compounds (panel a) and for groups of compounds based on their concentrations in the core tops relative to their

concentrations in the sediment traps (panel b) (all concentrations are normalized to g dry sediment, as in Table S1).

Figure 7: Relative offsets in δ^2H_{Lipid} values between *n*-$C_{16:0}$ fatty acid and phytol (blue triangles), sterol and phytol (orange diamonds), and *n*-$C_{16:0}$ fatty acid and sterol (brown squares), represented in terms of ε ($\varepsilon_{Lipid\ 1\text{-}Lipid\ 2} = (((\delta^2H_{Lipid\ 1} + 1000)/ (\delta^2H_{Lipid\ 2} + 1000)) -1) * 1000$). Sediment trap and core top values from Swiss lakes are plotted relative to total phosphorus concentrations (panels a and b). *T. pseudonana* values (panel c) are calculated from δ^2H_{Lipid} values are from chemostats grown at constant growth rates at different light levels (Sachs et al., 2017). Shading represents 95% confidence intervals of linear regressions. Regression lines are only shown for significant correlations ($p < 0.05$).

References

Boltz D. F. and Mellon M. G. (1948) Spectrophotometric determination of phosphate as molydiphosphoric acid. *Anal. Chem.* **20**, 749-751.

Brittingham A., Hren M. T. and Hartman G. (2017) Microbial alteration of the hydrogen and carbon isotopic composition of *n*-alkanes in sediments. *Org. Geochem.* **107**, 1-8.

Canuel E. A. and Martens C.S. (1996) Reactivity of recently deposited organic matter: Degradation of lipid compounds near the sediment–water interface. *Geochim. Cosmochim. Acta* **60**, 1793–1806.

Castañeda I. S. and Schouten S. (2011) A review of molecular organic proxies for examining modern and ancient lacustrine environments. *Quat. Sci. Rev.* **30**, 2851-2891.

Chivall D., M'Boule D., Sinke-Schoen D., Sinninghe Damsté J. S., Schouten S. and van der Meer M. T. J. (2014) The effects of growth phase and salinity on the hydrogen isotopic composition of alkenones produced by coastal haptophyte algae. *Geochim. Cosmochim. Acta* **140**, 381–390.

Craig H. and Gordon L. (1965) Deuterium and oxygen 18 variations in the ocean and the marine atmosphere. In *Proceedings of a Conference on Stable Isotopes in Oceanographic Studies and Paleotemperatures* (ed E. Tongiori). CNR-Laboratorio di Geologia Nucleare, Pisa. pp. 9-130.

Dansgaard W. (1964) Stable isotopes in precipitation. *Tellus* **16**, 436–468.

Diefendorf A. F., Freeman K. H., Wing S. L. and Graham, H.V. (2011). Production of *n*-alkyl lipids in living plants and implications for the geologic past. *Geochim. Cosmochim. Acta* **75**, 7472-7485.

Eisenreich W., Bacher A., Arigoni D. and Rohdich F. (2004) Biosynthesis of isoprenoids via the non-mevalonate pathway. *Cell. Mol. Life Sci.* **6**, 1401-1426.

Feakins S. J., Bentley L. P., Salinas N., Shenkin A., Blonder B., Goldsmith G. R., Ponton C., Arvin L. J., Wu M. S., Peters T., West A. J., Martin R. E., Enquist B. J., Asner G. P. and Malhi Y. (2016) Plant leaf wax biomarkers capture gradients

in hydrogen isotopes of precipitation from the Andes and Amazon. *Geochim. Cosmochim. Acta* **182**, 155-172.
Freimuth E. J., Diefendorf A. F. and Lowell T. V. (2017) Hydrogen isotopes of *n*-alkanes and *n*-alkanoic acids as tracers of precipitation in a temperate forest and implications for paleorecords. *Geochim. Cosmochim. Acta* **206**, 166-183.
Gao L., Edwards E. J., Zeng Y. and Huang Y. (2014) Major Evolutionary Trends in Hydrogen Isotope Fractionation of Vascular Plant Leaf Waxes. PLoS ONE **9**(11): e112610.
Gat J. R. (1996) Oxygen and hydrogen isotopes in the hydrologic cycle. *Annu. Rev. Earth Planet. Sci.* **24**, 225–262.
Haddad R. I., Martens C. S. and Farrington J. W. (1992) Quantifying early diagenesis of fatty acids in a rapidly-accumulating coastal marine sediment. *Org. Geochem.* **19**, 205–216.
Heinzelmann S. M., Villanueva L., Sinke-Schoen D., Sinninghe Damsté J. S., Schouten S. and van der Meer M. T. J. (2015) Impact of metabolism and growth phase on the hydrogen isotopic composition of microbial fatty acids. *Front. Microbio.* **6**, 408.
Heinzelmann S. M., Bale N. J., Villanueva L., Sinke-Schoen D., Philippart C. J. M., Sinninghe Damsté J. S., Smede J., Schouten S. and van der Meer M. T. J. (2016) Seasonal changes in the D/H ratio of fatty acids of pelagic microorganisms in the coastal North Sea. *Biogeosci.* **13**, 5527-5539.
Ho E. S. and Meyers, P.A. (1994) Variability of early diagenesis in lake sediments: Evidence from the sedimentary geolipid record in an isolated tarn. *Chem. Geo.* **112**, 309–324.
Hollander D. J., McKenzie J. A. and Ten Haven H. L. (1992) A 200 year sedimentary record of progressive eutrophication in Lake Greifen (Switzerland): implications for the origin of organic-carbon-rich sediments. *Geology* **20**, 825-828.
Hou J., D'Andrea W. J. and Huang Y. (2008) Can sedimentary leaf waxes record D/H ratios of continental precipitation? Field, model, and experimental assessments. *Geochim. Cosmochim. Acta* **72**, 3503-3517.
Huang Y., Shuman B., Wang Y. and Webb III T. (2002) Hydrogen isotope ratios of palmitic acid in lacustrine sediments record late Quaternary climate variations. *Geology* **30**, 1103-1106.
Huang Y., Shuman B., Wang Y. and Webb III T. (2004) Hydrogen isotope ratios of individual lipids in lake sediments as novel tracers of climatic and environmental change: a surface sediment test. *J. Paleolim.* **31**, 363-375.
Jensen J. P., Jeppesen E., Orlik K. and Kristensen P. (1994) Impact of nutrients and physical factors on the shift from cyanobacterial to chlorophyte dominance in shallow Danish lakes. *Can. J. Fish. Aquat. Sci.* **51**, 1692-1699.
Kahmen A., Hoffmann B., Schefuss E., Arndt S. K., Cernusak L. A., West J. B. and Sachse D. (2013) Leaf water deuterium enrichment shapes leaf wax n-alkane δD values of angiosperm plants II: Observational evidence and global implications. *Geochim. Cosmochim. Acta* **111**, 50–63.
Kawamura K., Ishiwatari R. and Ogura K. (1987) Early diagenesis of organic matter in the water column and sediments: Microbial degradation and resynthesis of lipids in Lake Haruna. *Org. Geochem.* **11**, 251–264.
Kornilova O. and Rosell-Melé A. (2003) Application of microwave-assisted extraction to the anaylsis of biomarker climate proxies in marine sediments. *Org. Geochem.* **34**, 1517-1523.

Ladd S. N. and Sachs J. P. (2015) Influence of salinity on hydrogen isotope fractionation in *Rhizophora* mangroves from Micronesia. *Geochim. Cosmochim. Acta* **168**, 206–221.

Ladd S. N., Dubois N. and Schubert C. J. (2017) Interplay of community dynamics, temperature, and productivity on the hydrogen isotope signatures of lipid biomarkers. *Biogeosci.* **14**, 3979-3994.

Li C., Sessions A. L., Kinnaman F. S. and Valentine D. L. (2009) Hydrogen-isotopic variability in lipids from Santa Barbara Basin sediments, *Geochim. Cosmochim. Acta* **73**, 4803-4823.

Lichtenthaler H. K. (1999) The 1-Deoxy-D-Xylulose-5-Phosphate pathway of isoprenoid biosynthesis in plants. *Ann. Rev. Plant Physiol. Plant Mol. Biol.* **50**, 47-65.

Lotter A. F., Sturm M., Teranes J. L. and Wehrli B. (1997) Varve formation since 1885 and high-resolution varve analysis in hypertrophic Baldeggersee (Switzerland). *Aquat. Sci.* **59**, 304-325.

Maloney A. E., Shinneman A. L., Hemeon K. and Sachs J. P. (2016) Exploring lipid 2 H/1 H fractionation mechanisms in response to salinity with continuous cultures of the diatom *Thalassiosira pseudonana*, *Org. Geochem.* **101**, 154-165.

M'boule, D., Chivall, D., Sinke-Schoen, D., Sinninghe Damsté, J. S., Schouten, S. and van der Meer M. T. J. (2014) Salinity dependent hydrogen isotope fractionation in alkenones produced by coastal and open ocean haptophyte algae, *Geochim. Cosmochim. Acta* **130**, 126–135.

Meyers, P. A. and Ishiwatari R. (1993) Lacustrine organic geochemistry: An overview of indicators of organic matter sources and diagenesis in lake sediments. *Org. Geochem.* **20**, 867–900.

Meyers P. A. and Takeuchi N. (1981) Environmental changes in Saginaw Bay, Lake Huron recorded by geolipid contents of sediments deposited since 1800. *Environ. Geol.* **3**, 257-266.

Miller M. B., Haubrich B. A., Wang Q., Snell W. J. and Nes W. J. (2012) Evolutionarily conserved $\Delta^{25(27)}$-olefin ergosterol biosynthesis pathyway in the alga *Chlamydomonas reinhardtii*. *J. Lipid Res.* **53**, 1636-1645.

Monchamp M.-E., Spaak P., Domaizon I., Dubois N., Bouffard D. and Pomati F. (2018) Homogenization of lake cyanobacterial communities over a century of climate change and eutrophication. *Nat. Ecol. Evol.* **2**, 317-324.

Morris I., Yentsch C. M. and Yentsch C. S. (1971) Relationship between light carbon dioxide fixation and dark carbon dioxide fixation by marine algae. *Limnol. Oceanogr.* **16**, 854-858.

Nelson D. B. and Sachs J. P. (2014) The influence of salinity on D/H fractionation in dinosterol and brassicasterol from globally distributed saline and hypersaline lakes. *Geochim. Cosmochim. Acta*, **133**, 325–339.

Nelson D. B. and Sachs J. P. (2016) Galápagos hydroclimate of the Common Era from paired microalgal and mangrove biomarker $^{2}H/^{1}H$ values. *Proc. Natl. Acad. Sci.* **113**, 3476-3481.

Nelson D. B., Ladd S. N., Schubert C. J. and Kahmen A. (2018) Rapid atmospheric transport and large-scale deposition of recently synthesized plant waxes. *Geochim. Cosmochim. Acta*. **222**, 599-617.

Osburn M. R., Sessions A. L., Pepe-Ranney C. and Spear J. R. (2011) Hydrogen-isotopic variability in fatty acids from Yellowstone National Park hot spring microbial communities. *Geochim. Cosmochim. Acta* **75**, 4830-4845, 2011.

Osburn M. R., Dawson K. S., Fogel M. L. and Sessions A. L. (2016) Fractionation of

hydrogen isotopes by sulphate- and nitrate-reducing bacteria. *Front*. *Microbio*. **7**, 1166m.

Pearson A., McNichol A. P., Benitez-Nelson B. C., Hayes J. M. and Eglinton. T. I. (2001) Origins of lipid biomarkers in Santa Monica Basin surface sediment: A case study using compound-specific $\Delta^{14}C$ analysis. *Geochim*. *Cosmochim*. *Acta* **65**, 3123-3137.

Pomati F., Matthews B., Jokela J., Schildknecht A. and Iberlings B. W. (2011) Effects of re-oligotrophication and climate warming on plankton richness and community stability in a deep mesotrophic lake. *Oikos* **121**, 1317-1327.

Rach O., Brauer A., Wilkes H. and Sachse D. (2014) Delayed hydrological response to Greenland cooling at the onset of the Younger Dryas in western Europe. *Nat*. *Geosci*. **7**, 109-112.

Rach O., Kahmen A., Brauer A. and Sachse D. (2017) A dual-biomarker approach for quantification of changes in relative humidity from sedimentary lipid D/H ratios. *Clim*. *Past* **13**, 741-757.

Randlett M. E., Bechtel A., van der Meer M. T. J., Peterse F., Litt T., Pickarski N., Kwiecien O., Stockhecke M., Wehrli B. and Schubert C. J. (2017) Biomarkers in Lake Van sediments reveal dry conditions in eastern Anatolia during 110.000–10.000 years BP. *Geochem*. *Geophys*. *Geosy*. **18**, 571-583.

Sachs J. P. and Schwab V. F. (2011) Hydrogen isotopes in dinosterol from the Chesapeake Bay estuary. *Geochim*. *Cosmochim*. *Acta* **75**, 444–459.

Sachs J. P., Sachse D., Smittenberg R. H., Zhang Z., Battisti D. S. and Golubic S. 2009. Southward movement of the Pacific intertropical convergence zone AD 1400–1850. *Nature Geo*. **2**, 519–525.

Sachs J. P. (2014) Hydrogen isotope signatures in the lipids of phytoplankton. In: *Treatise on Geochemistry*, *2nd Edition* (eds: H. D. Holland and K. K. Turekian). Elsevier, Oxford, UK. Vol. 12, pp. 79-94.

Sachs J. P. and Kawka O. E. (2015) The influence of growth rate on 2 H/1 H fractionation in continuous cultures of the coccolithophorid *Emiliania huxleyi* and the diatom *Thalassiosira pseudonana*. *PloS one* **10**, e0141643.

Sachs J. P., Maloney A. E. and Gregersen J. (2017) Effect of light on 2H/1H fractionation in lipids from continuous cultures of the diatom *Thalassiosira pseudonana*. *Geochim*., *Cosmochim*., *Acta* **209**, 204-215.

Sachse D., Radke J. and Gleixner G. (2004) Hydrogen isotope ratios of recent lacustrine sedimentary *n*-alkanes record modern climate variability. *Geochim*. *Cosmochim*. *Acta* **68**, 4877-4889.

Sachse D., Billault I., Bowen G. J., Chikaraishi Y., Dawson T. E., Feakins S. J., Freeman K. H., Magill C. R., McInerney F. A., van der Meer M. T. J., Polissar P., Robins R. J., Sachs J. P., Schmidt H. L., Sessions A. L., White J. W. C., West. J. B. and Kahmen A. (2012) Molecular paleohydrology: interpreting the hydrogen-isotopic composition of lipid biomarkers from photosynthesizing organisms. *Annu*. *Rev*. *Earth Planet*. *Sci*. **40**, 212-249.

Sargent J. R., Gatten R. R. and McIntosh R. (1977) Wax esters in the marine environment – their occurrence, formation, transformation, and ultimate fates. *Mar*. *Chem*. **5**, 573-584.

Sauer P. E., Eglinton T. I., Hayes J. M., Schimmelmann A. and Sessions A. L. (2001) Compound-specific D/H ratios of lipid biomarkers from sediments as a proxy for environmental and climatic conditions. *Geochim*. *Cosmochim*. *Acta* **65**, 213-222.

Schouten S., Ossebaar J., Schreiber K., Kienhuis M. V. M., Langer G., Benthien A. and Bijma, J. (2006) The effect of temperature, salinity and growth rate on the

stable hydrogen isotopic composition of long chain alkenones produced by *Emiliania huxleyi* and *Gephyrocapsa oceanica*. *Biogeosci*. **3**, 113–119.
Schwab V. F., Garcin Y., Sachse D., Todou G., Séné O., Onana J., Achoundong G. and Gleixner G. (2015) Dinosterol δD values in stratified tropical lakes (Cameroon) are affected by eutrophication. *Org*. *Geochem*. **88**, 35-49.
Sessions A. L. (2016) Factors controlling the deuterium contents of sedimentary hydrocarbons. *Org*. *geochem*. **96**, 43-64.
Sessions A. L., Burgoyne T. W., Schimmelmann A. and Hayes J. M. (1999) Fractionation of hydrogen isotopes in lipid biosynthesis. *Org*. *Geochem*. **30**, 1193–1200.
Sinninghe Damsté J. S., van Dongen B. E., Rijpstra W. I. C., Schouten S., Volkman J. K. and Geenevasen J. A. J. (2001) Novel intact glycolipids in sediments from an Antarctic lake (Ace Lake). *Org*. *Geochem*. **32**, 321-332.
Smittenberg R. H., Saenger C., Dawson M. N. and Sachs J. P. (2011) Compound-specific D/H ratios of the marine lakes of Palau as proxies for West Pacific Warm Pool hydrologic variability. *Quatern*. *Sci*. *Rev*. **30**, 921-933.
Teranes J. L. and McKenzie J. A. (1999) Stable isotope response to lake eutrophication: Calibration of a high-resolution lacustrine sequence from Baldeggersee, Switzerland. *Limnol*. *Oceanogr*. **44**, 320-333.
Theodorou M. E., Elrifi I. R., Turpin D. H. and Plaxton W. C. (1991) Effects of phosphorus limitation on respiratory metabolism in the green alga *Selenastrum minutum*. *Plant Physiol*. **95**, 1089-1095.
Tilman D., Kilham S. S. and Kilham P. (1982) Phytoplankton community ecology: the role of limiting nutrients. *Ann*. *Rev*. *Ecol*. *Syst*. **13**, 349-372.
Tipple B. J., Berke M. A., Doman C. E., Khachaturyan S. and Ehleringer J. R. (2013) Leaf *n*-alkanes record the plant-water environment at leaf flush. *Proc*. *Natl*. *Acad*. *Sci*. **110**, 2659–2664.
van der Meer M. T. J., Benthien A., French K. L., Epping E., Zondervan I., Reichart G. J., Bijma J., Sinninghe Damsté J. S. and Schouten, S. (2015) Large effect of irradiance on hydrogen isotope fractionation of alkenones in *Emiliania huxleyi*. *Geochim*. *Cosmochim*. *Acta* **160**, 16-24.
Volkman J. K. (2003) Sterols in microorganisms. *Appl*. *Microbiol*. *Biotechnol*. **60**, 495–506.
Volkman J. K., Johns R. B., Gillian, F. T. and Perry G. J. (1980) Microbial lipids of an intertidal sediment – I. Fatty acids and hydrocarbons. *Geochim*. *Cosmochim*. *Acta* **44**, 1133-1143.
Vranová E., Coman D. and Gruissem W. (2013) Network analysis of the MVA and MEP pathways for isoprenoid synthesis. *Annu*. *Rev*. *Plant*. *Biol*. **64**, 665-700.
Watson S. B., McCauley E. and Downing J. A. (1997) Patterns in phytoplankton taxonomic composition across temperate lakes of differing nutrient status. *Limnol*. *Oceanogr*. **42**, 487-495.
Weiss G. M., Pfannerstill E. Y., Schouten S., Sinninghe Damsté J. S. and van der Meer, M. T. J. (2017) Effects of alkalinity and salinity at low and high light intensity on hydrogen isotope fractionation of long-chain alkenones produced by *Emiliania huxleyi*. *Biogeosci*. **14**, 5693-5704.
Wolhowe M. D., Prahl F. G., Langer G., Oviedo A. M. and Ziveri P. (2015) Alkenone δD as an ecological indicator: A culture and field study of physiologically-controlled chemical and hydrogen-isotopic variation in C_{37} alkenones. *Geochim*. *Cosmochim*. *Acta* **162**, 166-182.
Zarrouk W., Carrasco-Pancorbo A., Zarrouk M., Segura-Carretero A. and Fernandez-

1008 Gutierrez A. (2009) Multi-component analysis (sterols, tocopherols and
1009 triterpenic dialcohols) of the unsaponifiable fraction of vegetable oils by liquid
1010 chromatography– atmospheric pressure chemical ionization–ion trap mass
1011 spectrometry. *Talanta* **80**, 924–934.
1012 Zhang Z. and Sachs J. P. (2007) Hydrogen isotope fractionation in freshwater algae: 1.
1013 Variations among lipids and species. *Org*. *Geochem*. **38**, 582–608.
1014 Zhang X., Gillespie A. and Sessions A. L. (2009) Large D/H variations in bacterial
1015 lipids reflect central metabolic pathways. *Proc*. *Natl*. *Acad*. *Sci*. **106**, 12580-
1016 12586.
1017 Zhang Z., Sachs J. P., Marchetti A. (2009) Hydrogen isotope fractionation in
1018 freshwater and marine algae: II. Temperature and nitrogen limited growth rate
1019 effects. *Org*. *Geochem*. **40**, 428-439.
1020

Table 1

Table 1: Location and characteristics of the ten sampled lakes. Elevation, catchment area, surface area, and max depth from *Müller et al., 1998, Keller et al., 2008, and* https://www.lakepedia.com. Depth-integrated winter maximum phosphorus values from BAFU, Bern Building, Traffic, and Energy Directorate, and Lucerne Environment and Energy. Spring 2015 water isotopes are mean and one standard deviation from two to five depths within upper 20 m, with replicates from date of sediment trap deployment and retrieval. August 2015 water isotopes are mean and one standard deviation of 2 – 4 surface water samples collected from near the late shore.

Lake Name and Number in Figure 1	Lat. (°N)	Long. (°E)	Elevation (m)	Catchment Area (km^2)	Surface Area (km^2)	Max depth (m)	Trap Deployment Date (2015)	Trap Retrieval Date (2015)	Sed. Acc. rate (cm Yr^{-1})	Winter maximum P (µg/L)	Water δ^2H (‰, VSMOW), spring 2015	Water $\delta^{18}O$ (‰, VSMOW), spring 2015	Water δ^2H (‰, VSMOW), August 2015	Water $\delta^{18}O$ (‰, VSMOW), August 2015
1 – Baldegg	47.200	8.260	463	73	5	6	April 2	April 27	0.2	29	-61 ± 2	-8.4 ± 0.2	-62 ± 1	-8.2 ± 0.1
2 – Brienz	46.726	7.965	563	754	29	173	April 8	April 28	0.5	3	-94 ± 1	-12 ± 2	-99 ± 1	-14.1 ± 0.1
3 – Greifen	47.354	8.672	439	195	8	7	April 14	May 11	0.3	52	-68 ± 3	-9.3 ± 0.6	-68 ± 1	-9.1 ± 0.1
4 – Inkwil	47.199	7.664	461	2.13	0.12	4.6	April 10	April 27	2	22	-72 ± 3	-10.0 ± 0.4	-60 ± 1	-7.3 ± 0.1
5 – Lucerne	47.005	8.346	431	2223	110	120	April 15	May 4	0.2	6	-84 ± 2	-11.8 ± 0.2	-86 ± 1	-12.1 ± 0.1
6 – Mauen	47.171	8.076	504	4.3	0.6	7	April 16	May 12	0.7	26	-65 ± 2	-8.6 ± 0.2	-61 ± 1	-7.7 ± 0.1
7 – Rot	47.070	8.314	419	4.6	0.5	16	April 1	April 27	0.5	39	-80 ± 2	-11.2 ± 0.2	-77 ± 1	-10.4 ± 0.2
8 – Sarnen	46.869	8.219	469	194	7	15	April 7	April 28	2	5	-82 ± 1	-11.5 ± 0.2	-80 ± 2	-11.1 ± 0.2
9 – Soppen	47.090	8.081	596	1.59	0.23	26.5	April 16	May 12	0.9	106	-57 ± 2	-7.4 ± 0.2	-55 ± 1	-6.8 ± 0.1
10 – Thun	46.699	7.673	558	2504	46	52	April 8	April 29	0.9	3	-90 ± 2	-12.6 ± 0.2	-95 ± 1	-12.1 ± 0.1

Table 2

Table 2: $\alpha_{Lipid\text{-}Water}$ values for all compounds analyzed in core top (0-1 cm) samples. Values represent mean and one standard deviation of replicate measurements, with propagated uncertainties from water and lipid δ^2H measurements.

		***n*-alkanoic acids**											***n*-alkanols**						**isoprenoids**	
Lake Name and Number in Figure 1		**C14:0**	**C16:0**	**C16:1ω9**	**C18:0**	**C18:x**	**C20:0**	**C22:0**	**C24:0**	**C26:0**	**C28:0**	**C30:0**	**C14**	**C16**	**C20**	**C22**	**C24**	**C26**	**phytol**	**Brassicasterol**
1 – Baldegg	α	0.823	0.829	0.862	0.851	0.856	0.895	0.891	0.898	0.888	0.906	0.886	0.872	0.867	0.861	0.870	0.867	0.814	0.672	0.765
	1σ	0.005	0.003	0.004	0.003	0.004	0.007	0.006	0.003	0.002	0.002	0.003	0.004	0.003	0.007	0.005	0.003	0.002	0.005	0.002
3 – Greifen	α	0.849	0.832	0.814	0.869	0.835	0.893	0.894	0.903	0.898	0.912	0.903	0.848	0.861	0.853	0.874	0.889	0.834	0.645	0.748
	1σ	0.004	0.003	0.003	0.007	0.004	0.006	0.004	0.005	0.004	0.004	0.003	0.004	0.004	0.004	0.004	0.009	0.004	0.10	0.004
4 – Inkwil	α	0.867	0.850	0.845	0.867	0.851	0.905	0.906	0.908	0.900	0.913	0.901	0.912	0.938	0.906	0.898	0.894	0.856	0.690	0.762
	1σ	0.004	0.004	0.005	0.004	0.006	0.007	0.008	0.004	0.004	0.004	0.007	0.004	0.006	0.006	0.008	0.005	0.004	0.10	0.003
5 – Lucerne	α	0.842	0.847	0.878	0.876	0.862	0.906	0.917	0.921	0.919	0.918	0.924	0.899	0.886	0.876	0.864	0.893	0.864	0.662	0.798
	1σ	0.004	0.013	0.003	0.004	0.003	0.004	0.002	0.004	0.004	0.005	0.003	0.002	0.003	0.002	0.002	0.002	0.002	0.004	0.006
6 – Mauen	α	0.813	0.849	0.845	0.877	0.857	0.911	0.915	0.912	0.906	0.914	0.914	0.872	0.884	0.876	0.889	0.904	0.857	0.674	0.775
	1σ	0.004	0.004	0.006	0.005	0.010	0.006	0.004	0.005	0.005	0.005	0.007	0.004	0.003	0.004	0.009	0.005	0.002	0.011	0.003
7 – Rot	α	0.841	0.850	0.837	0.873	0.849	0.903	0.909	0.905	0.902	0.910	0.902	*N.A.*	0.861	0.878	0.880	0.883	0.849	0.672	0.762
	1σ	0.007	0.002	0.003	0.007	0.004	0.004	0.002	0.005	0.005	0.006	0.012		0.005	0.003	0.004	0.005	0.005	0.003	0.002
8 – Sarnen	α	0.872	0.855	0.888	0.874	0.883	0.900	0.900	0.895	0.902	0.913	0.906	0.895	0.895	0.887	0.889	0.895	0.849	0.684	0.798
	1σ	0.002	0.005	0.004	0.009	0.002	0.005	0.003	0.002	0.002	0.002	0.003	0.009	0.007	0.005	0.001	0.002	0.003	0.002	0.001
9 – Soppen	α	0.821	0.824	0.886	0.860	0.843	0.892	0.902	0.897	0.893	0.913	0.883	0.863	0.859	0.870	0.877	0.874	0.822	0.687	0.746
	1σ	0.003	0.003	0.003	0.003	0.004	0.007	0.004	0.002	0.003	0.003	0.005	0.003	0.003	0.003	0.003	0.005	0.004	0.003	0.004
10 – Thun	α	0.872	0.865	0.886	0.886	0.886	0.917	0.927	0.933	*N.A.*	*N.A.*	*N.A.*	*N.A.*	0.884	0.891	0.864	0.896	0.863	*N.A.*	0.822
	1σ	0.007	0.008	0.003	0.006	0.029	0.010	0.004	0.005					0.007	0.003	0.002	0.002	0.002		0.007

Table 3

Table 3: $\alpha_{Lipid\text{-}Water}$ values for all compounds analyzed in sediment trap samples. Values represent mean and one standard deviation of replicate measurements, with propagated uncertainties from water and lipid δ^2H measurements.

		***n*-alkanoic acids**						***n*-alkanols**					**isoprenoids**	
Lake Name and Number in Figure 1		**C14:0**	**C16:0**	**C16:1ω9**	**C18:0**	**C18:x**	**C18:3ω3**	**C14**	**C16**	**C20**	**C22**	**C24**	**Phytol**	**Brassica-sterol**
1 – Baldegg	α	0.819	0.827	0.836	0.848	0.855	*N.A.*	0.885	0.860	0.881	0.882	0.815	0.674	0.771
	1σ	0.001	0.002	0.013	0.011	0.001		0.006	0.007	0.004	0.003	0.006	0.003	0.003
2 – Brienz	α	0.815	0.813	0.811	0.857	0.846	*N.A.*	0.919	*N.A.*	0.925	0.916	0.871	0.647	0.794
	1σ	0.002	0.001	0.015	0.002	0.012		0.002		0.003	0.004	0.001	0.003	0.003
3 – Greifen	α	0.782	0.812	0.813	0.847	0.843	0.781	0.835	0.844	0.871	0.876	0.821	0.656	0.751
	1σ	0.002	0.002	0.006	0.002	0.003	0.001	0.001	0.001	0.003	0.010	0.001	0.006	0.001
4 – Inkwil	α	0.795	0.806	0.811	0.856	0.839	0.795	0.856	*N.A.*	0.871	0.877	0.844	0.656	0.752
	1σ	0.003	0.003	0.006	0.008	0.005	0.002	0.005		0.004	0.006	0.005	0.003	0.003
5 – Lucerne	α	0.788	0.795	0.783	0.859	0.866	0.813	*N.A.*	*N.A.*	*N.A.*	*N.A.*	0.863	0.636	0.801
	1σ	0.003	0.001	0.001	0.002	0.001	0.014					0.002	0.002	0.006
6 – Mauen	α	0.791	0.824	0.807	0.866	0.856	0.794	0.839	0.861	0.881	0.882	0.817	0.648	0.792
	1σ	0.002	0.002	0.004	0.013	0.008	0.013	0.001	0.005	0.004	0.001	0.002	0.002	0.005
7 – Rot	α	0.799	0.820	0.850	0.849	0.832	0.790	0.844	0.863	0.875	0.882	0.847	0.672	0.778
	1σ	0.004	0.002	0.005	0.003	0.003	0.001	0.003	0.001	0.001	0.002	0.005	0.011	0.022
8 – Sarnen	α	*N.A.*	0.839	0.864	0.891	0.883	*N.A.*	0.889	0.902	0.902	0.905	0.845	0.651	0.797
	1σ		0.001	0.005	0.016	0.003		0.018	0.008	0.003	0.006	0.002	0.006	0.003
9 – Soppen	α	0.808	0.805	0.846	0.848	0.824	0.787	0.853	0.895	0.908	0.862	0.811	0.689	0.741
	1σ	0.004	0.002	0.001	0.004	0.001	0.004	0.001	0.008	0.004	0.007	0.001	0.006	0.003
10 – Thun	α	0.820	0.805	0.813	0.874	0.858	0.857	*N.A.*	0.892	0.899	0.895	0.866	0.673	0.807
	1σ	0.003	0.001	0.004	0.012	0.013	0.004		0.017	0.004	0.006	0.006	0.004	0.003

Table 4

Table 4: $\varepsilon_{Lipid\text{-}Lipid}$ values from core tops and sediment traps. Values are reported with 1σ based on propagated errors from individual lipid δ^2H measurements

	Sediment Traps			Core Tops		
Lake Name and Number in Figure 1	$\varepsilon_{C16:0\text{-}Phytol}$	$\varepsilon_{Brass\text{-}Phytol}$	$\varepsilon_{C16:0\text{-}Sterol}$	$\varepsilon_{C16:0\text{-}Phytol}$	$\varepsilon_{Brass\text{-}Phytol}$	$\varepsilon_{C16:0\text{-}Sterol}$
1 – Baldegg	227 ± 11	144 ± 6	72 ± 9	232 ± 10	137 ± 9	84 ± 3
2 – Brienz	257 ± 15	227 ± 7	23 ± 12	*N.A.*	*N.A.*	*N.A.*
3 – Greifen	238 ± 20	144 ± 11	82 ± 14	290 ± 20	159 ± 19	113 ± 5
4 – Inkwil	229 ± 10	147 ± 3	71 ± 9	231 ± 18	103 ± 16	116 ± 3
5 – Lucerne	251 ± 14	260 ± 11	-7 ± 12	279 ± 21	205 ± 12	61 ± 18
6 – Mauen	270 ± 15	221 ± 8	40 ± 13	260 ± 22	150 ± 20	96 ± 5
7 – Rot	219 ± 21	158 ± 38	53 ± 30	264 ± 6	134 ± 5	115 ± 3
8 – Sarnen	290 ± 19	225 ± 15	53 ± 13	250 ± 8	165 ± 2	72 ± 6
9 – Soppen	180 ± 15	77 ± 11	96 ± 10	198 ± 6	86 ± 7	104 ± 6
10 – Thun	*N.A.*	*N.A.*	14 ± 21	*N.A.*	*N.A.*	53 ± 18

Figure 1

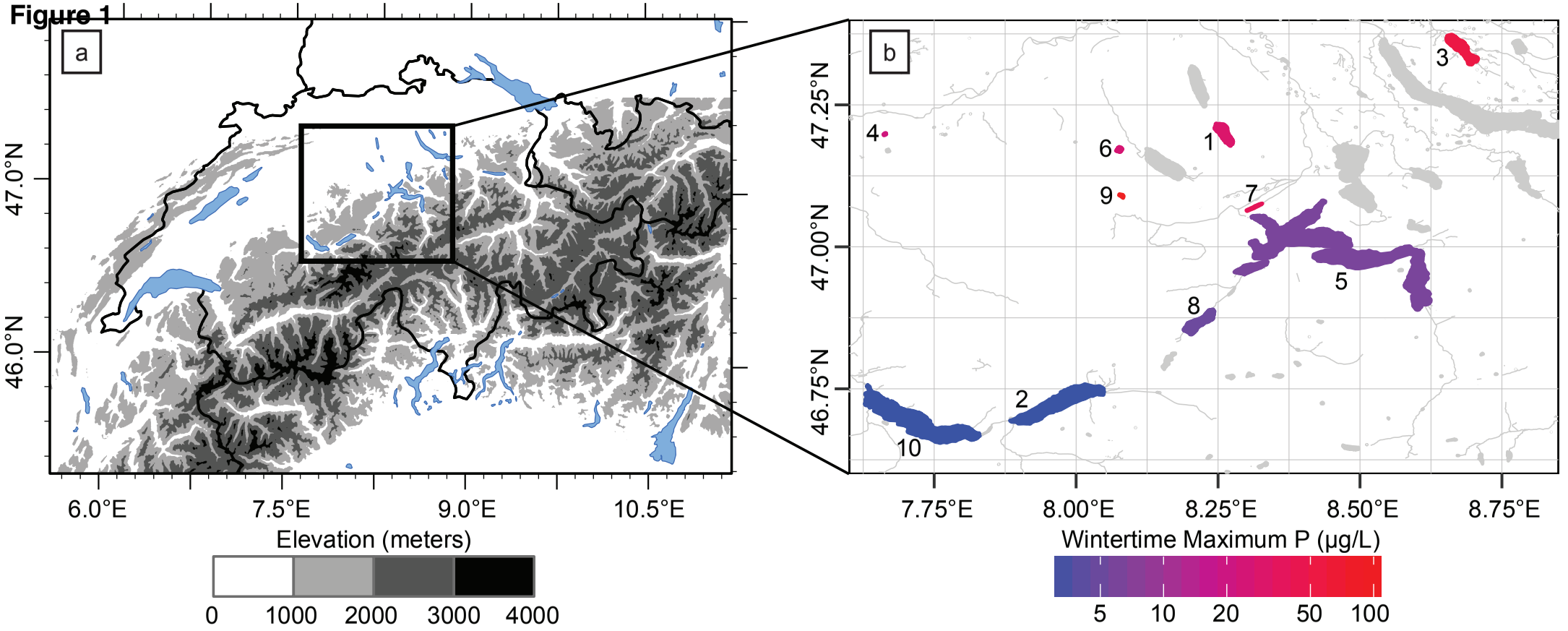
a
b
47.0°N
46.0°N
6.0°E
7.5°E
9.0°E
10.5°E
Elevation (meters)
0
1000
2000
3000
4000
47.25°N
47.00°N
46.75°N
7.75°E
8.00°E
8.25°E
8.50°E
8.75°E
1
2
3
4
5
6
7
8
9
10
Wintertime Maximum P (µg/L)
5
10
20
50
100

Figure 2

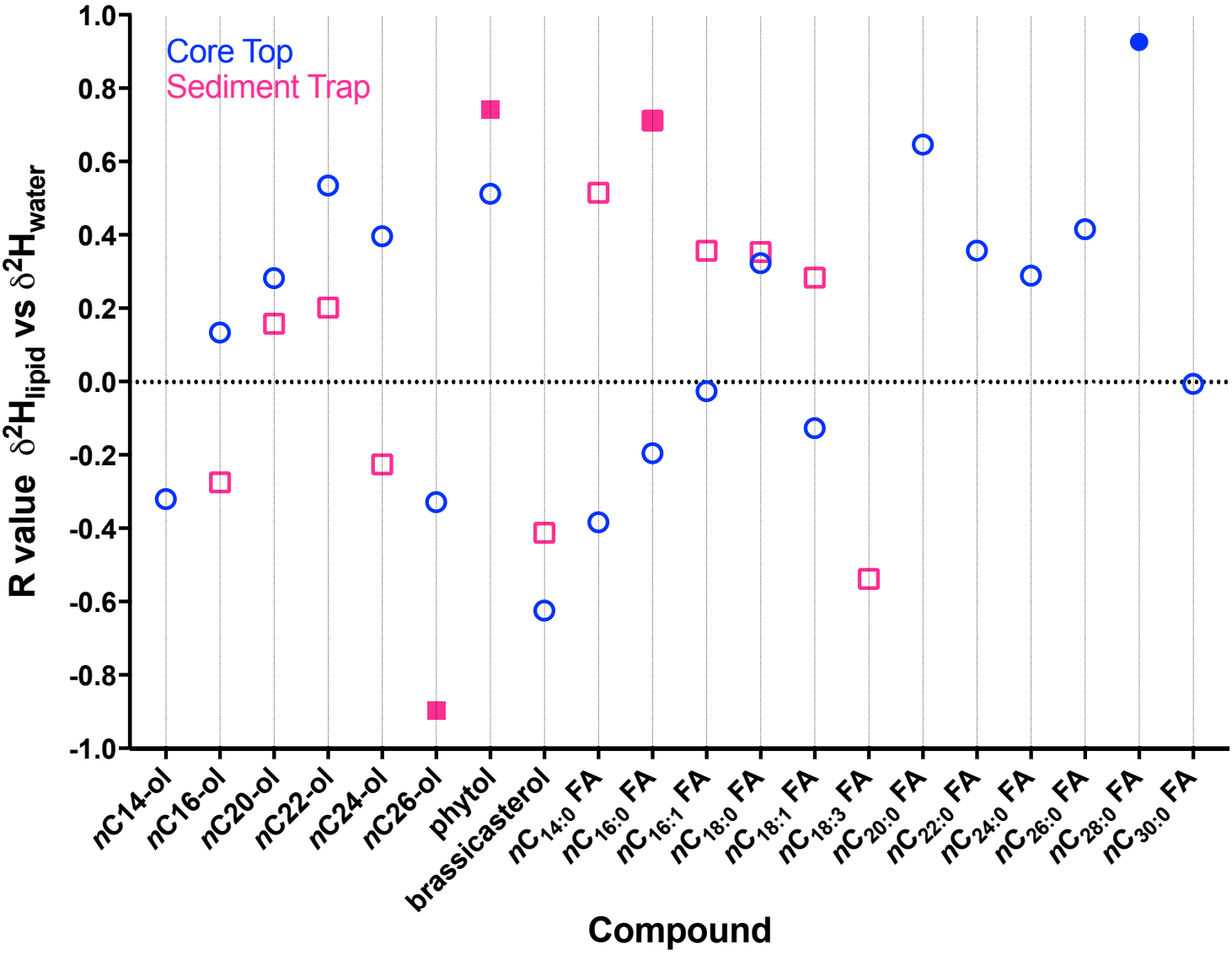
Core Top
Sediment Trap
R value δ^2H_{lipid} vs δ^2H_{water}
1.0
0.8
0.6
0.4
0.2
0.0
-0.2
-0.4
-0.6
-0.8
-1.0
nC14-ol
nC16-ol
nC20-ol
nC22-ol
nC24-ol
nC26-ol
phytol
brassicasterol
$nC_{14:0}$ FA
$nC_{16:0}$ FA
$nC_{16:1}$ FA
$nC_{18:0}$ FA
$nC_{18:1}$ FA
$nC_{18:3}$ FA
$nC_{20:0}$ FA
$nC_{22:0}$ FA
$nC_{24:0}$ FA
$nC_{26:0}$ FA
$nC_{28:0}$ FA
$nC_{30:0}$ FA
Compound

Figure 3

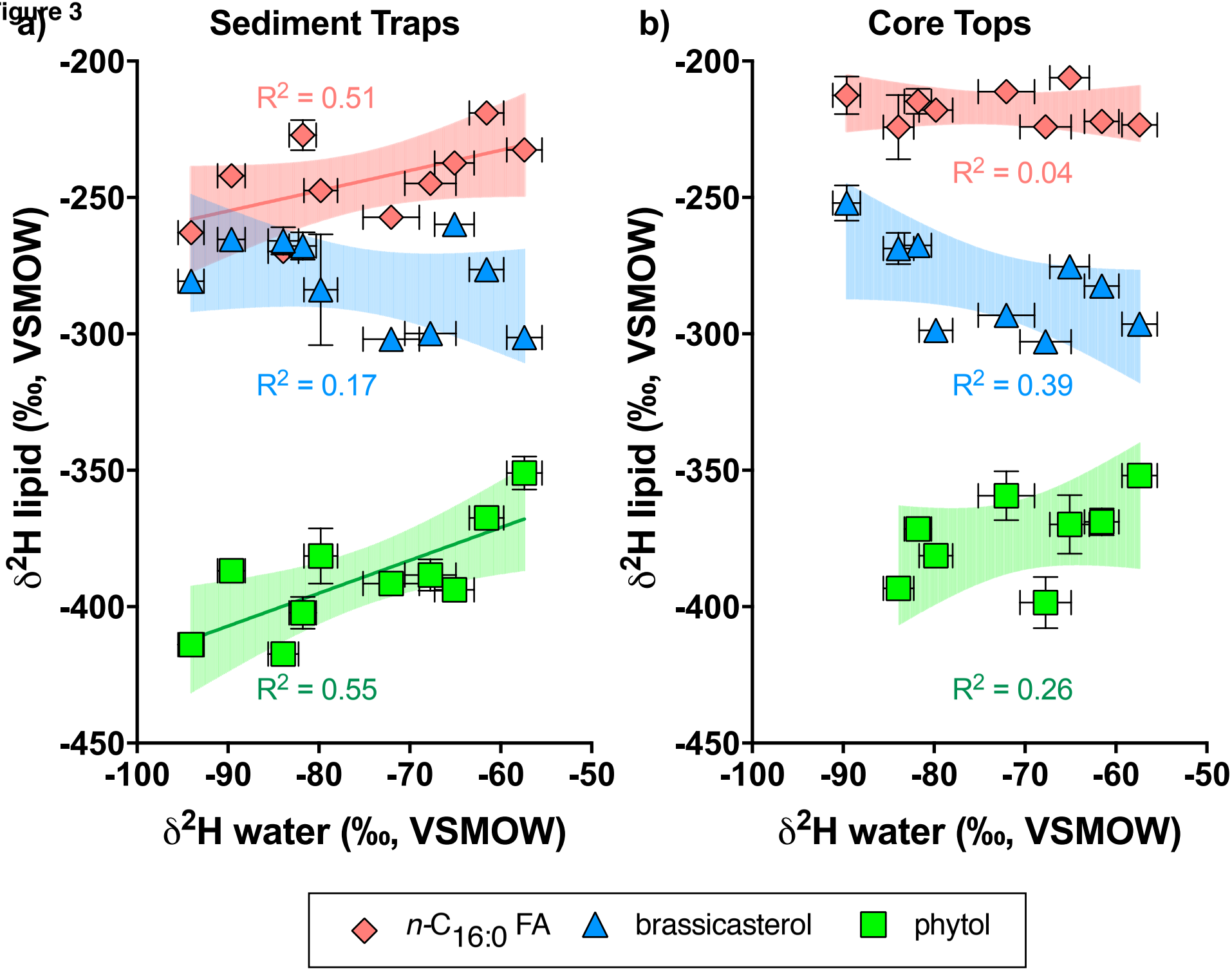
a)
Sediment Traps
b)
Core Tops
-200
-250
-300
-350
-400
-450
δ²H lipid (‰, VSMOW)
R² = 0.51
R² = 0.17
R² = 0.55
R² = 0.04
R² = 0.39
R² = 0.26
-100
-90
-80
-70
-60
-50
δ²H water (‰, VSMOW)
n-C16:0 FA
brassicasterol
phytol

Figure 4

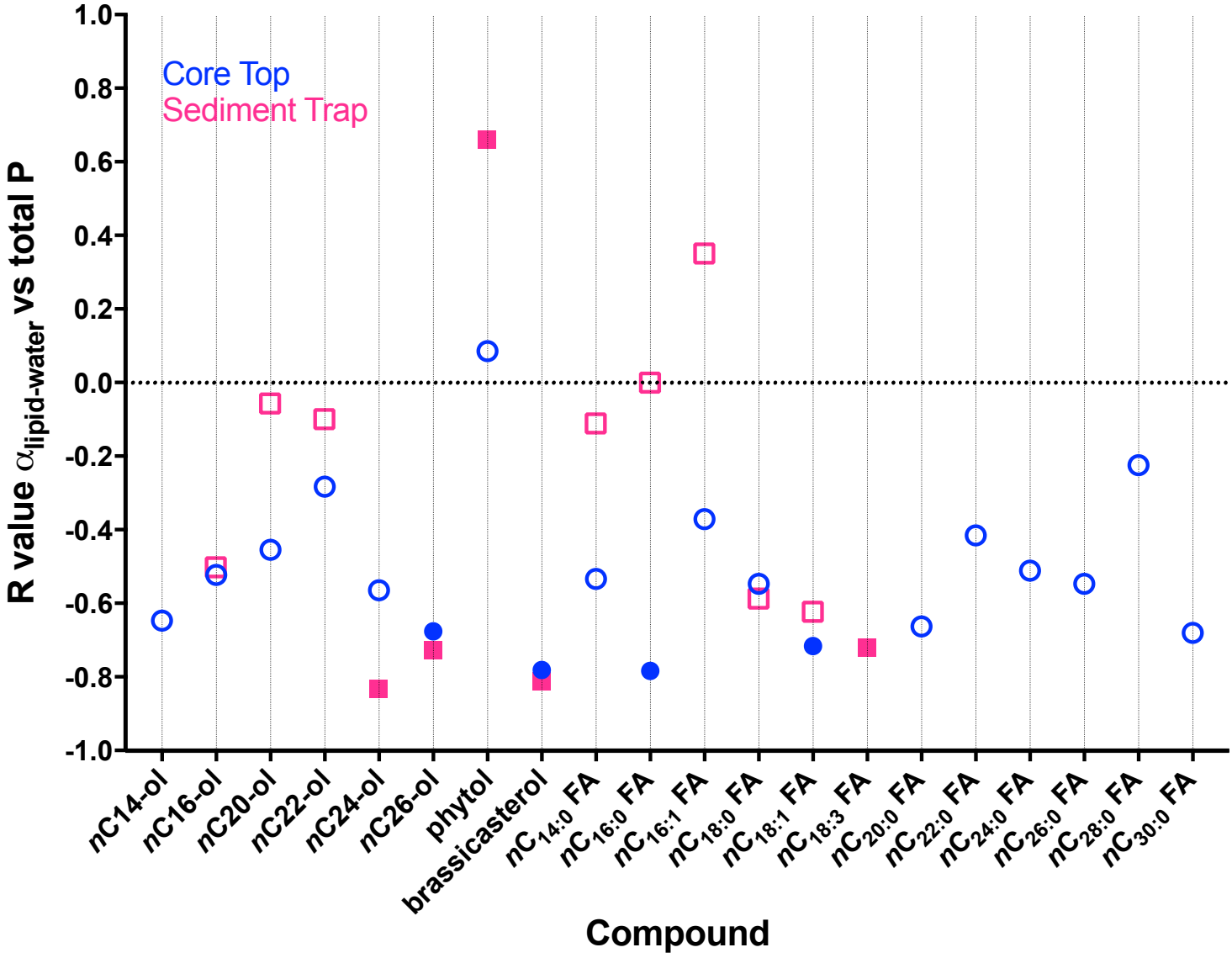
Core Top
Sediment Trap
R value $\alpha_{lipid\text{-}water}$ vs total P
1.0
0.8
0.6
0.4
0.2
0.0
-0.2
-0.4
-0.6
-0.8
-1.0
nC14-ol
nC16-ol
nC20-ol
nC22-ol
nC24-ol
nC26-ol
phytol
brassicasterol
$nC_{14:0}$ FA
$nC_{16:0}$ FA
$nC_{16:1}$ FA
$nC_{18:0}$ FA
$nC_{18:1}$ FA
$nC_{18:3}$ FA
$nC_{20:0}$ FA
$nC_{22:0}$ FA
$nC_{24:0}$ FA
$nC_{26:0}$ FA
$nC_{28:0}$ FA
$nC_{30:0}$ FA
Compound

Figure 5

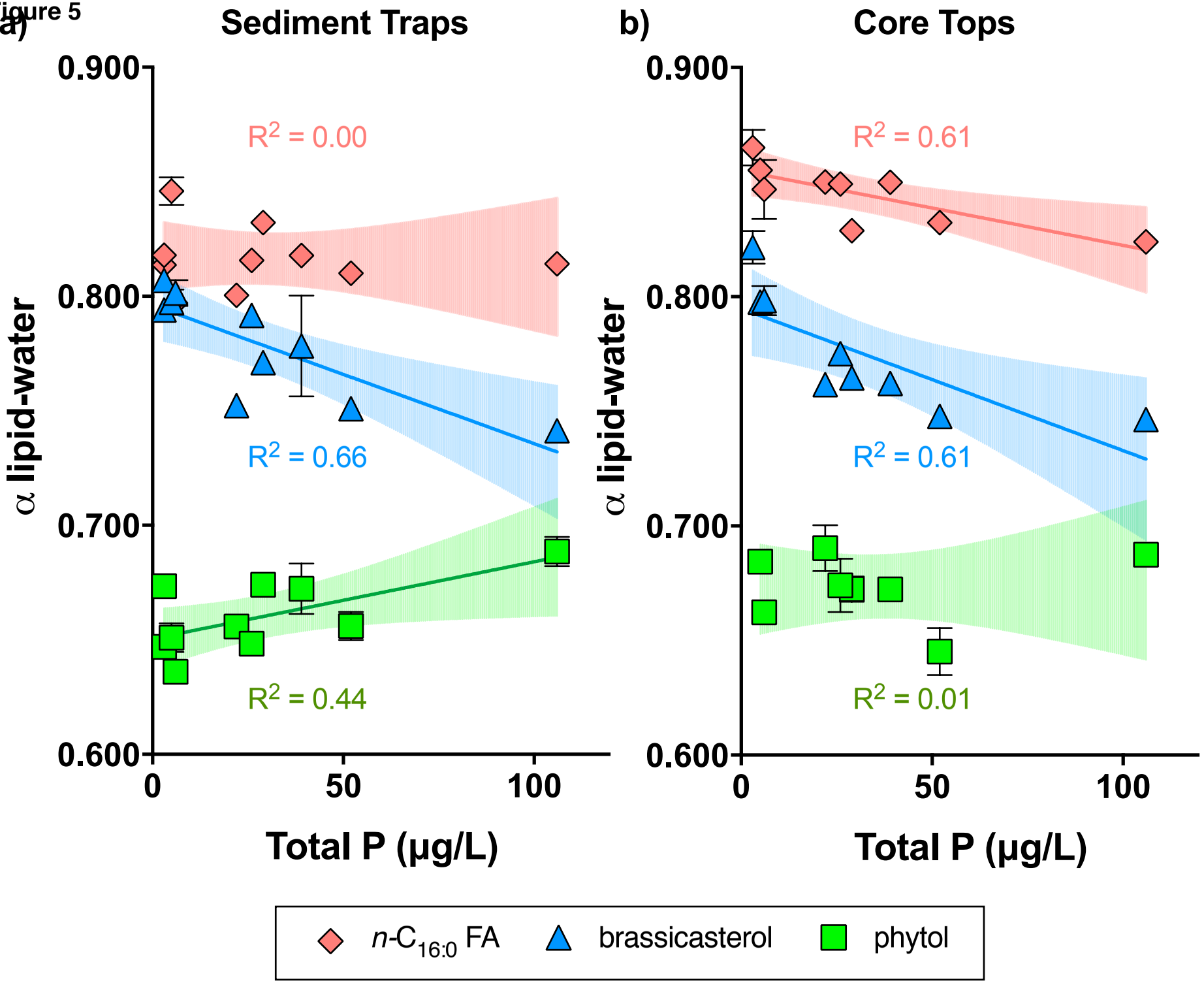
a)
Sediment Traps
b)
Core Tops
0.900
0.800
0.700
0.600
α lipid-water
R2 = 0.00
R2 = 0.66
R2 = 0.44
R2 = 0.61
R2 = 0.61
R2 = 0.01
0
50
100
Total P (µg/L)
n-C16:0 FA
brassicasterol
phytol

Figure 6

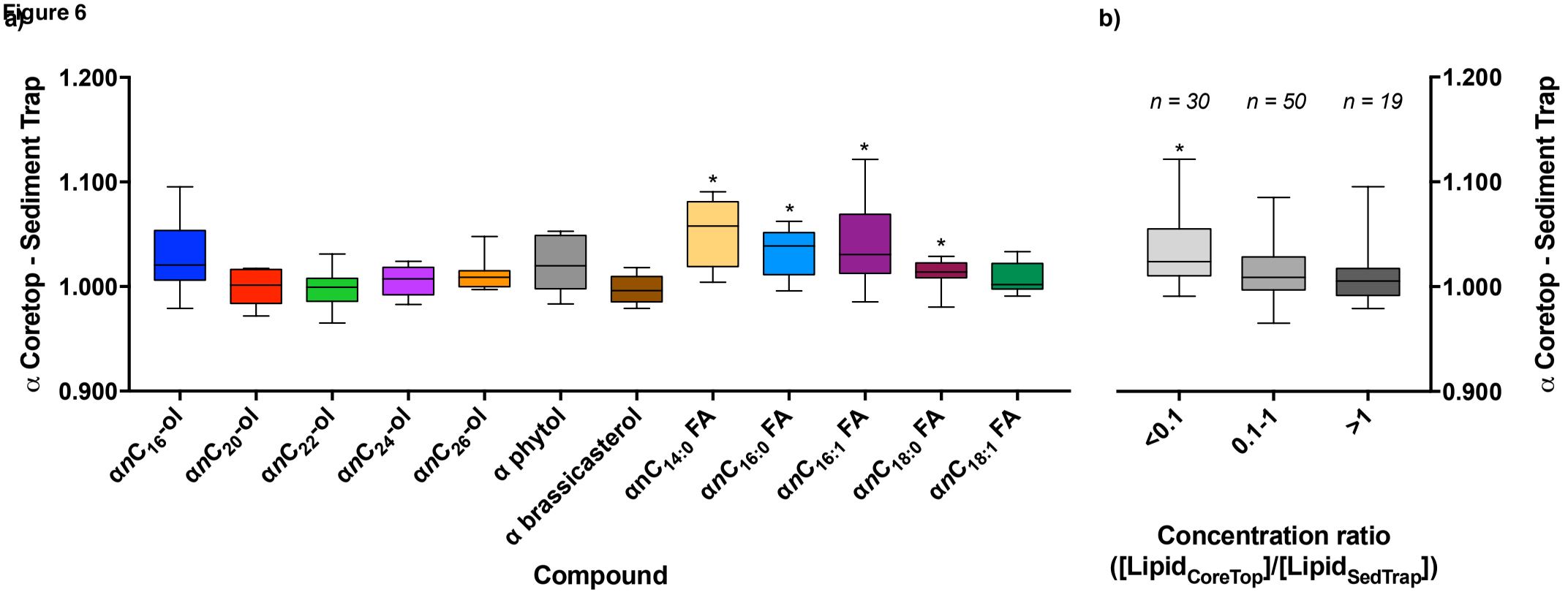
a)
b)
α Coretop - Sediment Trap
1.200
1.100
1.000
0.900
αnC16-ol
αnC20-ol
αnC22-ol
αnC24-ol
αnC26-ol
α phytol
α brassicasterol
αnC14:0 FA
αnC16:0 FA
αnC16:1 FA
αnC18:0 FA
αnC18:1 FA
Compound
n = 30
n = 50
n = 19
<0.1
0.1-1
>1
Concentration ratio
([Lipid CoreTop]/[Lipid SedTrap])

Figure 7

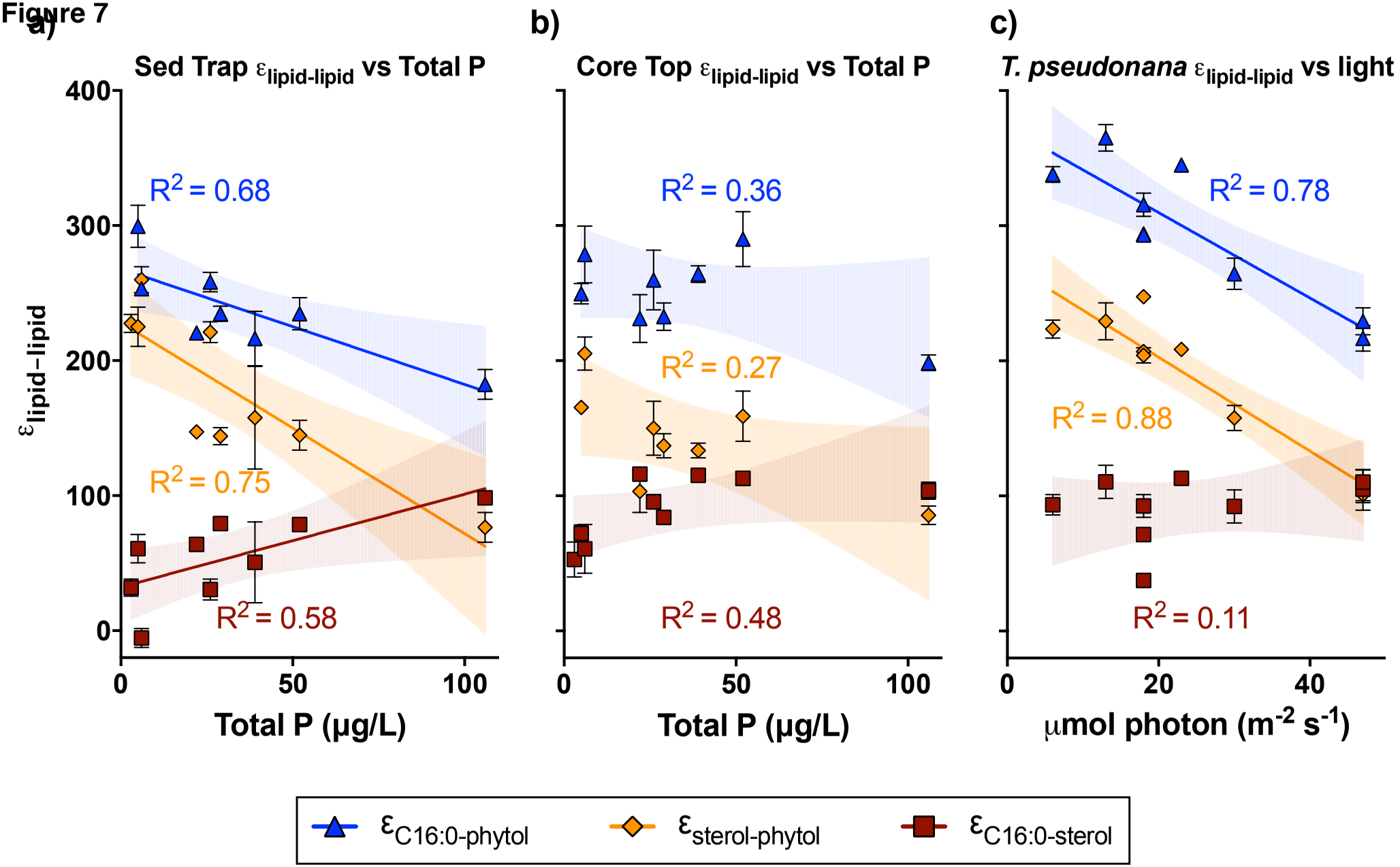
a)
Sed Trap $\varepsilon_{lipid-lipid}$ vs Total P
b)
Core Top $\varepsilon_{lipid-lipid}$ vs Total P
c)
T. pseudonana $\varepsilon_{lipid-lipid}$ vs light
$\varepsilon_{lipid-lipid}$
R^2 = 0.68
R^2 = 0.75
R^2 = 0.58
R^2 = 0.36
R^2 = 0.27
R^2 = 0.48
R^2 = 0.78
R^2 = 0.88
R^2 = 0.11
0
100
200
300
400
0
50
100
Total P (µg/L)
0
50
100
Total P (µg/L)
0
20
40
µmol photon (m^{-2} s^{-1})
$\varepsilon_{C16:0-phytol}$
$\varepsilon_{sterol-phytol}$
$\varepsilon_{C16:0-sterol}$